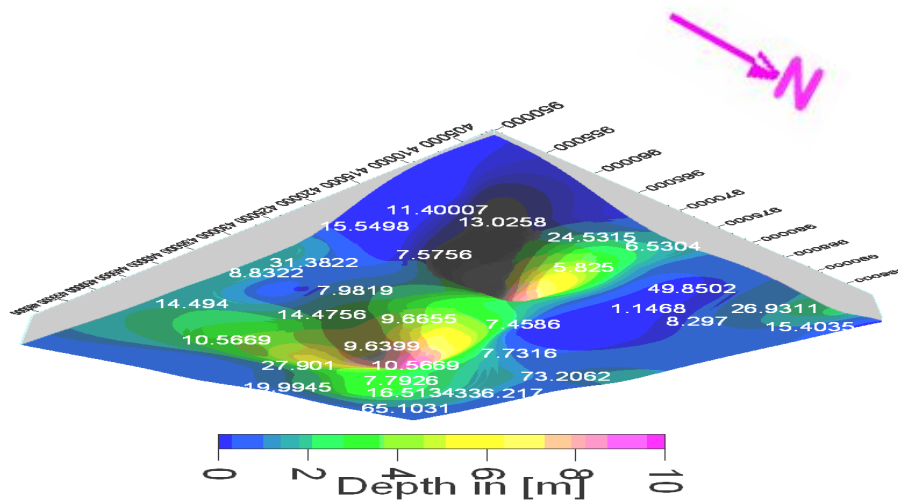


**ADDIS ABABA UNIVERSITY**  
**SCHOOL OF GRADUATED STUDIES**



***GEOELECTRICAL INVESTIGATION FOR THE ASSESSMENT OF  
GROUND WATER DISTRIBUTIONS IN BECHO PLAIN, SOUTH WEST  
SHOWA***



By

**BIRHAN MUCHE**

**Research Advisor: Dr. SHIMELES FISSEHA**

**October 2008**

**ADDIS ABABA UNIVERSITY**

**SCHOOL OF GRADUATED STUDIES**

***GEOELECTRICAL INVESTIGATION FOR THE ASSESSMENT OF  
GROUND WATER DISTRIBUTIONS IN BECHO PLAIN, SOUTH WEST  
SHOWA***

***A THESIS SUBMITTED TO THE SCHOOL OF GRADUATE STUDIES  
OF ADDIS ABABA UNIVERSITY IN PARTIAL FULFILLMENT OF  
THE REQUIREMENTS FOR THE DEGREE OF MASTER OF SCIENCE IN  
EXPLORATION GEOPHYSICS.***

**By**

**BIRHAN MUCHE**

**October,2008**

**Research Advisor: Dr. SHIMELES FISSEHA**

**ADDIS ABABA UNIVERSITY**

**SCHOOL OF GRADUATED STUDIES**

***GEOELECTRICAL INVESTIGATION FOR THE ASSESSMENT OF  
GROUND WATER DISTRIBUTIONS IN BECHO PLAIN, SOUTH WEST  
SHOWA***

**By**

**BIRHAN MUCHE**

**October 2008**

**DEPARTMENT OF EARTH SCIENCE**

Name

Signature

Dr. Balemwal Atnafu -----

-----

Chairman, Department Graduate Committee

Dr. Shimeles Fisseha-----

-----

Research Advisor

Dr. Getnet Mewa -----

-----

External Examiner

Dr. Abera Alemu -----

-----

Internal Examiner

## **DEDICATION**

*This Thesis work is dedicated to Almaz Muche.  
My elder sister, I will see you in the eternal world.*

*I trust God*

## **ACKNOWLEDGEMENTS**

The present study has been conducted in the context of Becho plain ground water resources evaluation and development, for irrigation project. I am mostly grateful to the Water Works Design and Supervision that provide for this work their raw VES data, TEM Processed data, geological and hydrogeological information.

It is a great pleasure to put forward my gratitude for my advisor Dr.Shimeles Fisseha. He has shown his humble and compassionate personality for me and he helped me systematically and analytically to handle all my thesis work . In addition, he took me to the different field works; he guided well me to get a better performance and editing this manuscript. In addition,I would like to thank his students Tatek Asefa and Menegesha Sisay.

Undeniably, I would like to express my gratefulness to Dr Tigistu Haile who paved a way for my thesis work creating a first hand exposure of preparing model of thesis in well-log course.

I thank Dr.Atalay Ayele and his students particularly, Binyam Beyene and Baxter Chimlambe Who helped me in providing computer.

I wish success of Awassa Teacher Education College and its administration staff visions, which offer me sponsorship to upgrade my qualification. I would like to thank, Ato Assefa Adane (ACTE lecturer) who encourages me to continue my education and his best advices.

I want to praise Jesus who does not let me alone and makes me to be the triumphant through all my tribulations and temptations.

I thank every body, who made it possible for me to complete this thesis work.

## **ABSTRACT**

This thesis work deals with the regional interpretation of electrical resistivity sounding, survey, carried out in the Becho plain, Southwest Showa. The principal objective is to study the ground water conditions such as depth to the water table, thickness and lateral boundaries of aquifer and possible flow direction. Parametric Transient Electromagnetic, sounding were also conducted at test borehole sites for calibration and comparison purpose. The geophysical survey was part of an integrated geotechnical work conducted by Water Works Design and Supervision Enterprise.

The focus of this thesis work is interpretation thirty-one Schlumberger soundings with a maximum current electrode spacing ranging from 1.5m to 1000m, from Becho plain and the surrounding area, and one Transient electromagnetic sounding, at Asgorie test well site.

Interpretation of these soundings indicates the presence of a likely alluvial aquifer of 240m maximum depth and other water-bearing volcanic rocks, at the SW boarder the Becho plain. These volcanic aquifers show variable thickness and formation resistivity depending on composition and degree of saturation.

Possible fault line is indicated in the eastern central part of the survey area and intrusion of volcanic rocks is identified near to the boarder line of southern part, possibly it may be the weak zone. In general, four geoelectrical layers are identified in this thesis work. These are the top layer, alluvium, aquifer and bedrocks. The top layer consists of mostly clay and silt. The alluvial consists of unconsolidated sediment such as sand, gravel and silt. The aquifer consists of unconsolidated sediment such as gravel, silt and in some part the basalt. The bedrock is consists of mostly basalt, ryyolite, and ignimbrite and fracture basalt.

## Table of content

<b>ACKNOWLEDGEMENT</b> .....	<b>I</b>
<b>ABSTRACT</b> -----	<b>II</b>
LIST OF TABLES-----	VI
<b>CHAPTER ONE</b> .....	<b>1</b>
<b>1. INTRODUCTION</b> .....	<b>1</b>
1.1 GENERAL.....	1
1.2 THE STUDY AREA.....	1
<b>1.2.1 LOCATION, TOPOGRAPHY AND ACCESSIBILITY</b> .....	<b>1</b>
<b>1.2.2 REGIONAL GEOLOGY</b> .....	<b>3</b>
<b>1.2.3 TECTONICS</b> .....	<b>4</b>
1.2.4 .....	5
1.2.5 <i>Hydrogeological conditions of Becho plain</i> .....	6
1.3. STATEMENT OF THE PROBLEM AND MAIN OBJECTIVES .....	7
1.3.1 <i>Statement of the problems</i> .....	7
1.3.2 <i>Objectives and the scope of the study:</i> .....	8
<b>CHAPTER TWO</b> .....	<b>9</b>
<b>2.1. THE PRINCIPLE OF GEOELECTRICAL METHODS IN GEOPHYSICAL EXPLORATION</b> .....	<b>9</b>
2.1.1 <i>Static electromagnetic fields</i> .....	10
2.1.2 <i>Quasi-stationary electromagnetic fields</i> .....	10
2.1.3 <i>Resistivity of rocks</i> .....	11
2.1.4 <i>Dielectric permittivity</i> .....	12
2.2. VERTICAL ELECTRICAL SOUNDING AND APPARENT RESISTIVITY .....	12
2.2.1 ELECTRODE CONFIGURATIONS AND GEOMETRIC FACTORS.....	12
2.2.1 <i>Transformation of Wenner to Schlumberger apparent resistivity over layered earth</i> .....	22
2.2.2 <i>Comparison of Dipole-dipole, Schlumberger, Square and Wenner electrode arrays</i> .....	24
2.2.3 <i>Schematic presentation of eight electrode configurations considered</i> .....	24
2.3 TIME DOMAIN ELECTROMAGNETIC SOUNDING .....	25
2.3.1 <i>Sources of error in TEM measurements</i> .....	28
2.3.2 <i>Ground water exploration</i> .....	32
2.3.3 THE COMPARISON BETWEEN TEM AND VES .....	33
<b>CHAPTER THREE</b> .....	<b>34</b>
<b>3. GEOPHYSICAL SURVEY AT BECHO-PLAIN</b> .....	<b>34</b>
3.1 VERTICAL ELECTRICAL SOUNDING .....	34
3.1.1 <i>Source Data</i> .....	34
3.1.2 <i>Instrumentation</i> .....	34
<b>3.1.3 DATA PROCESSING AND PRESENTATION OF RESISTIVITY SURVEY</b> .....	<b>35</b>
3.2 TRANSIENT ELECTROMAGNETIC METHOD (TEM) .....	35
3.2.1 <i>Data acquisition of Transient Electromagnetic Method (TEM)</i> .....	35

3.2.2 DATA PROCESSING AND PRESENTATION OF TEM SURVEYS.....	36
<b>FIG 3.1 THE DISTRIBUTION OF VES AND TEM ON THE SURVEY AREA .....</b>	<b>39</b>
<b>CHAPTER FOUR .....</b>	<b>40</b>
<b>4. RESULT AND INTERPRETAION.....</b>	<b>40</b>
<b>4.1 QUALITATIVE APPROACH .....</b>	<b>40</b>
<b>4.1.1 QUALITATIVE APPROACH FOR THE STACKED PLOT .....</b>	<b>41</b>
<b>4.2 QUANTITATIVE AND SEMI-QUANTITATIVE INTERPRETATIONS. ....</b>	<b>44</b>
4.2.1 Semi-quantitative interpretations of the 1-D geoelectric sections .....	44
4.3 THE OVERALL GEOELECTRIC PICTURE OF THE STUDY AREA.....	46
<b>5.1 CONCLUSIONS.....</b>	<b>48</b>
<b>5.2 RECOMMENDATIONS .....</b>	<b>49</b>
<b>REFERENCES .....</b>	<b>50</b>
<b>DECLARATION.....</b>	<b>52</b>
<b>ANNEX.....</b>	<b>52</b>
<b>A.1 MEASURING THE CURRENT PENETRATION DEPTH .....</b>	<b>53</b>
<b>A.2 THE 3-D GEOELECTRICAL SECTION FOR THE RESPECTIVE FOUR LAYERS .....</b>	<b>53</b>
<b>A.3 QUANTITATIVE AND SEMIQUANTITATIVE INTERPRETATION TEM .....</b>	<b>53</b>
<b>A.4 QUANTITATIVE AND SEMIQUANTITATIVE INTERPRETATION THE SUBSURFACE LAYERS IN 3-D GEOELECTRICAL SECTIONS OF VES.....</b>	<b>53</b>
<b>A.5 THE 2-D GEOELECTRICAL SECTION.....</b>	<b>53</b>
<b>A.6 GLOSSARY .....</b>	<b>53</b>
A.5.1 GEOPHYSICS TERMS .....	53
<b>A.7 THE INVERTED DATA PLOTS AND THEIR CORRESPONDING RESULTS.....</b>	<b>53</b>
<b>A.1 MEASURING THE CURRENT PENETRATION DEPTH.....</b>	<b>54</b>
<b>A.2 THE 3-D GEOELECTRICAL SECTION FOR THE RESPECTIVE FOUR LAYERS .....</b>	<b>55</b>
<b>A.3 QUANTITATIVE AND SEMIQUANTITATIVE INTERPRETATION TEM.....</b>	<b>57</b>
<b>A.4 QUANTITATIVE AND SEMIQUANTITATIVE INTERPRETATION THE SUBSURFACE LAYERS IN 3-D GEOELECTRICAL SECTIONS OF VES .....</b>	<b>58</b>
<b>A.5 THE 2-D GEOELECTRICAL SECTION.....</b>	<b>60</b>
<b>A.6 GLOSSARY .....</b>	<b>61</b>
A.6.1 GEOPHYSICS TERMS .....	61
A.6.2 HYDROGEOLOGICAL CONCEPTS AND TERMS .....	62

<b>FIGURE A.7 THE INVERTED DATA PLOTS AND THEIR.....</b>	<b>64</b>
<b>CORRESPONDING RESULTS .....</b>	<b>64</b>
<b>VESB1 .....</b>	<b>67</b>

**List of figures**

<i>Fig 1.1: Location map of Becho plain. -----</i>	<i>2</i>
<i>Fig 1.2: Digital topographic model of central Ethiopia, showing the location of Becho plain.-----</i>	<i>3</i>
<i>Fig1.3: The geological map of Becho-----</i>	<i>6</i>
<i>Fig 1.4: The hydrological map of the study area-----</i>	<i>7</i>
<i>Fig 2.1: The four electrodes array for measuring earth resistivity-----</i>	<i>13</i>
<i>Fig 2.2: A single current source. -----</i>	<i>14</i>
<i>Fig 2.3: Four electrodes linear array. -----</i>	<i>19</i>
<i>Fig 2.4: The eight electrode configurations-----</i>	<i>25</i>
<i>Fig 2.5 : The time-domain EM wave forms-----</i>	<i>27</i>
<i>Fig 2.6: The form of eddy current that propagates down ward and out ward like smoke rings at successive interval of time-----</i>	<i>28</i>
<i>Figure 2.7 : Central loop induction method for carrying out Time-Domain electromagnetic-----</i>	<i>29</i>
<i>Fig 2.8: Grounded wire source method for carrying out Time –Domain electromagnetic method-----</i>	<i>29</i>
<i>Fig 3.1 :The distribution of VES and TEM On the survey area.....-----</i>	<i>39</i>
<i>Figure 4.1: Stacked plan map of apprent resistivity of Becho plain-----</i>	<i>41</i>
<i>Figure 4.2: Apparent resistivity plan map at pseudo depth of <math>AB/2 = 750m</math>-----</i>	<i>43</i>
<i>Figure 4.3: Interpreted geo-electric layers along profile A-A'-----</i>	<i>45</i>
<i>Figure 4.4: Interpreted geo-electric layers along profile BB'-----</i>	<i>45</i>
<i>Figure 4.5: Interpreted geo-electric layers along profile C-C-----</i>	<i>46</i>

<i>FigA.1.1: Correlation between depth of current penetration and current electrodes spacing AB/2-----</i>	<i>46</i>
<i>Fig A.2.1: The 3-D geoelectrical section of the first layer-----</i>	<i>55</i>
<i>Fig A.2.2: The 3-D geoelectrical section of second layer-----</i>	<i>55</i>
<i>Fig A.2.3: The 3-D geoelectrical section of the third layer-----</i>	<i>56</i>
<i>Fig A.2.4: The 3-D geoelectrical section of the fourth layer Depth (Infinite depth) -----</i>	<i>56</i>
<i>Fig A.3.1 (a) apparent resistivity versus delay time (b) 1-D geoelectrical section of inverted result of (a) and (c) the corresponding geological interpretation of TEM-----</i>	<i>58</i>
<i>Fig A.4.1: Sub surfacelayers in NS and WE parts of the aquifers, depth and resistivity values are given in this plot-----</i>	<i>59</i>
<i>Figure A.5.1: Along the profile B-B'-----</i>	<i>60</i>
<i>Figure A.5.2: Along the profile A-A'-----</i>	<i>62</i>
<i>Figure A.7 the inverted data plots and their corresponding results-----</i>	<i>66-69</i>

## **List of Tables**

<i>Table 2.1 The comparison between Dipole, Schlumberger, Square and Wenner according to the criteria listed-----</i>	<i>24</i>
<i>Table 2.2 The comparison between the advantage and the disadvantage of TEM and VES-----</i>	<i>33</i>
<i>Table 3.1 Range of the resistivity values of major geological formations-----</i>	<i>47</i>

# CHAPTER ONE

## 1. INTRODUCTION

### 1.1 GENERAL

Water Works Design and Supervision Enterprise (WWDSE) are under taking ground water assessment on the consultancy basis in Becho plain, in the vicinity of Addis Ababa. The evaluation of ground water potential of Becho and other adjacent plains were major undertakings by Ministry of Water Resource as a client.

Geophysical investigations, as a major component of the multi –disciplinary study, were carried out to supplement the on going work by giving some additional subsurface geological and hydrological information. This manuscript presents the geophysical component of this integrated study as part of the thesis project for postgraduate program in exploration geophysics of the department of Earth science at Addis Ababa University. This thesis is organised in five chapters.

The first chapter is introduction and presents a general insight on the location, geology and hydro-geological setup of the project area. The general and specific objectives and the scope of the study are also presented in the first chapter. Chapter two discusses the basic principles of the geophysical methods which are used for this study. Chapter three presents the data processing and interpretation procedures. Chapter four contains discussions of the main results and interpretations. Finally, conclusions and recommendations of this study are given in chapter five.

### 1.2 The study area

#### 1.2.1 Location, Topography and Accessibility

The Becho plain lies in southwest showa in the Oromia Regional State. The elevation variations of the survey area is from 2040 to 2120m above mean sea level. The approximate geographical coordinates are  $38^{\circ}08'E - 38^{\circ}36'E$  and  $8^{\circ}38'N - 9^{\circ}00'N$ . The Becho plain ground water basin is reached along the Addis Ababa – Jima high way at approximately 13km to 90 km distance from AddisAbaba.

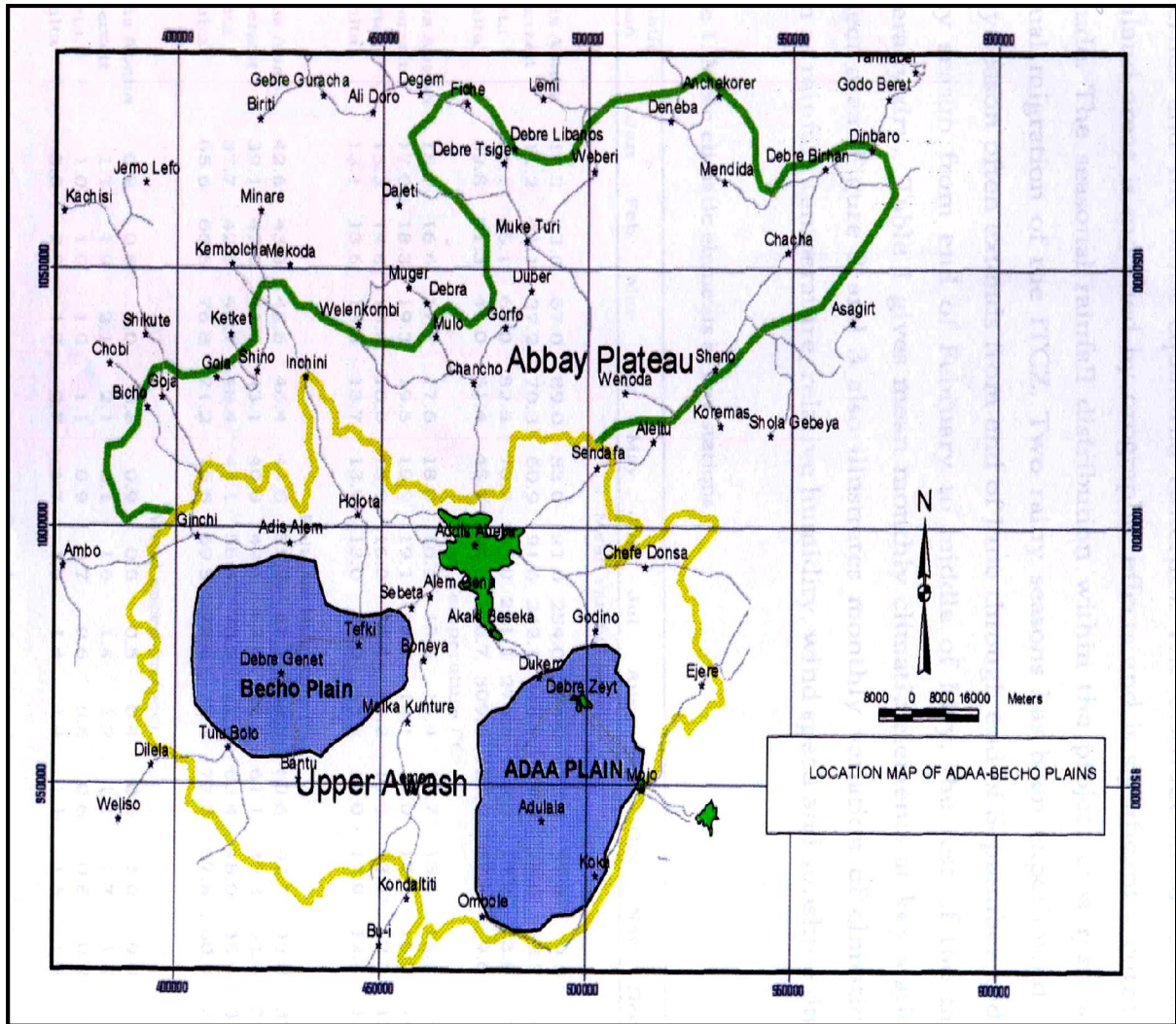
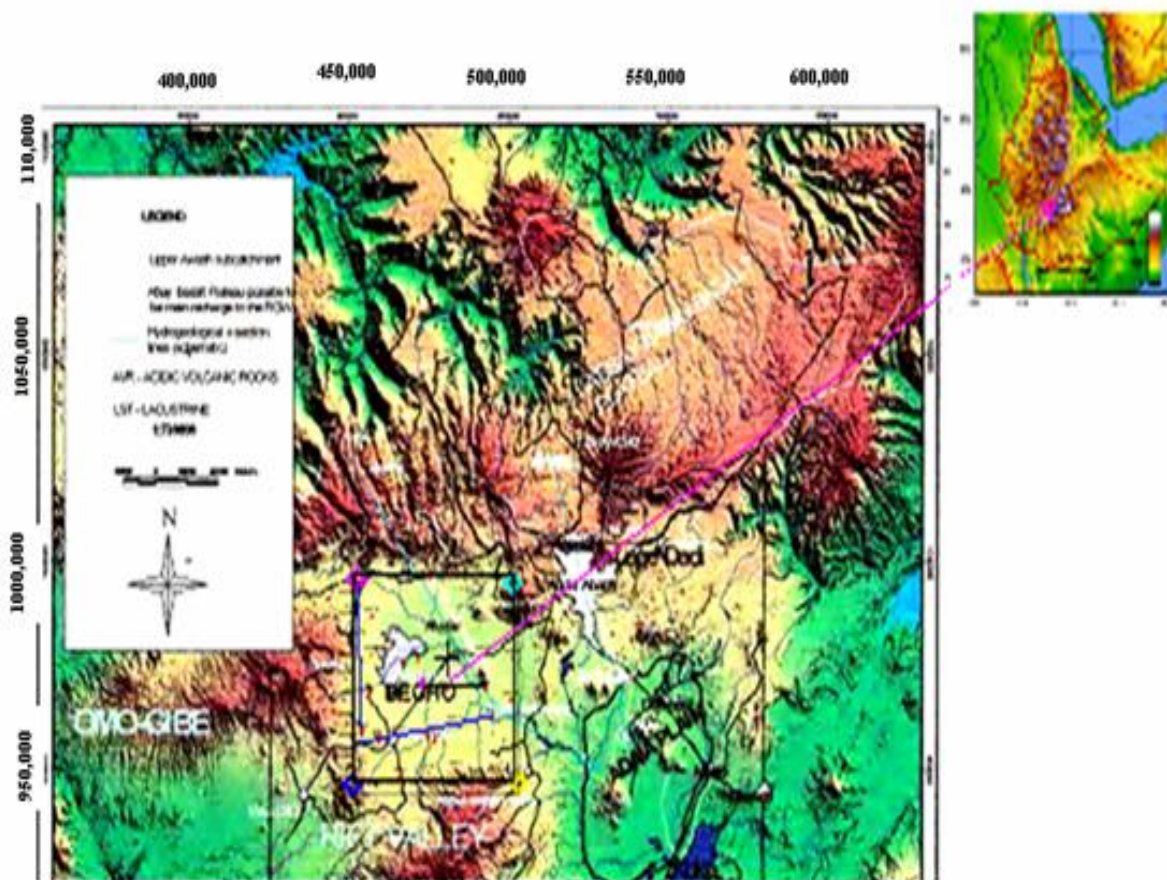


Figure 1.1: Location map of Becho plain.



▲----- The VES points. ◆ ----The TEM position.

Figure 1.2: Digital topographic model of central Ethiopia, showing the location of Becho plain and Ethiopia Topography map . The profiles and VES points are indicated.

### 1.2.2 Regional Geology

The basement rocks of Ethiopia consist of Precambrian igneous and metamorphics containing several orogenic episodes. It is in these rocks or from these rocks that the majority of economic mineral deposits exists. These include gold deposits of the northern, western and southern provinces, copper, zinc and lead sulphides in greenschist facies metamorphics, talc and nickel and platinum in the Welega Province. The basement rocks are relatively impermeable and thus water resources are in general only associated with fracturing and faulting resulting from rift development of the Red Sea and East African-Ethiopian Rift Valley. Northern provinces where deposits partly of glacial origin have been noted. subsidence followed in the Mesozoic with a

large shallow sea spreading initially over the Ogaden province eventually extending further north and west as the land continued to subside. This sequence was followed by general uplift and drying out of lake beds to leave gypsum and anhydrite precipitates.

Similar cycles continued through the Tertiary. Regional tectonic activity associated with rifting events in the Red Sea, Gulf of Aden and East African Rift Valley during the late Tertiary caused faulting and fracturing together with widespread volcanism. Vast quantities of basaltic lava was extruded over the western half of Ethiopia. This was accompanied by ash and coarser tephra forming a sequence known as the Trap Series. Several shield volcanoes consisting of alkali basalts and tephra developed at this time around the eastern edge of the Lake Tana depression.

Quaternary deposits are mainly confined to those associated with large depressions and lakes. Seismic and volcanic activity continues today along the Ethiopian Rift valley system.

The regional geology of the area is characterized by a series of formation and events from early Tertiary to Quaternary era. The grand Afro-Arabian swell was formed in upper Eocene. Following uplift of the horn of Africa, immense quantities of lavas, the Trap series, extruded from fissure and eruption centers from the fissure and eruption center (Mohr, 1961).

The trap series lavas, which are mostly basaltic in composition (with some acidic flows in the upper parts), cover large areas of Mesozoic sediments and in some places; they rest directly on the basement complex.

Such uplifts, together with extrusion of thick and extensive trapean lava, account for the formation of the present high land region of Ethiopia.

In the upper Pliocene to recent, a succession of pantelleritic Rhyololites, Trachytes and Ignimbrites with subordinate intermediate and basic rocks, were erupted chiefly at the rift margins and along the seismically active Wonji fault. This trachyte-pantelleritic ignimbrite covered most of the southern Ethiopia plateau and filled main Ethiopia Rift. Its thickness range from about 300m to 500m, Probably even greater on the rift floor.

### **1.2.3 Tectonics**

The Tertiary-Quaternary system, known as the East Africa system, is one of the largest structural features of the earth crust. It is widely believed that diverging lithospheric plates have formed them, since early Tertiary times. It extends from Mozambique to Syria. The East Africa system is the most typically developed in the section as the main Ethiopia Rift (Mohr,

1964), which extends from lake Chamo, in the south, to Afar in the north. The main Ethiopian Rift is characterized by NE-SW, and ENE-WSW, trending normal (faults) are predominantly trending NE-SW with dip towards NW and SE respectively

#### 1.2.4 Geological background of Becho plain.

From the geological point of view, Becho is situated in alluvial zone of south western of Addis Ababa. The rhyolites in Becho plain forms isolated cones. Obsidian up to 10 cm across is common in the pick of the cones. Data on the ages of the rhyolites are not available; however, from the cross-cutting relationship they can be younger than the adjacent ignimbrite. The ignimbrite outcropps in most part of the plain. It is composed of welded tuff (ignimbrite) and non-welded pyroclastics fall (ash and tuff). It is grayish to white in colour and when welded, it exhibits fiamine textures, elongated rock fragments of various colour. Around the legedadi plain and melka kulture area, the thickness of this unite reaches up to 200m (exploration drill data). In the Becho plain area, this is covered by thin (5-7m) thick residual soil developed from the same rocks. The age of this unit is estimated from 5.11- to - 3.26 Ma.

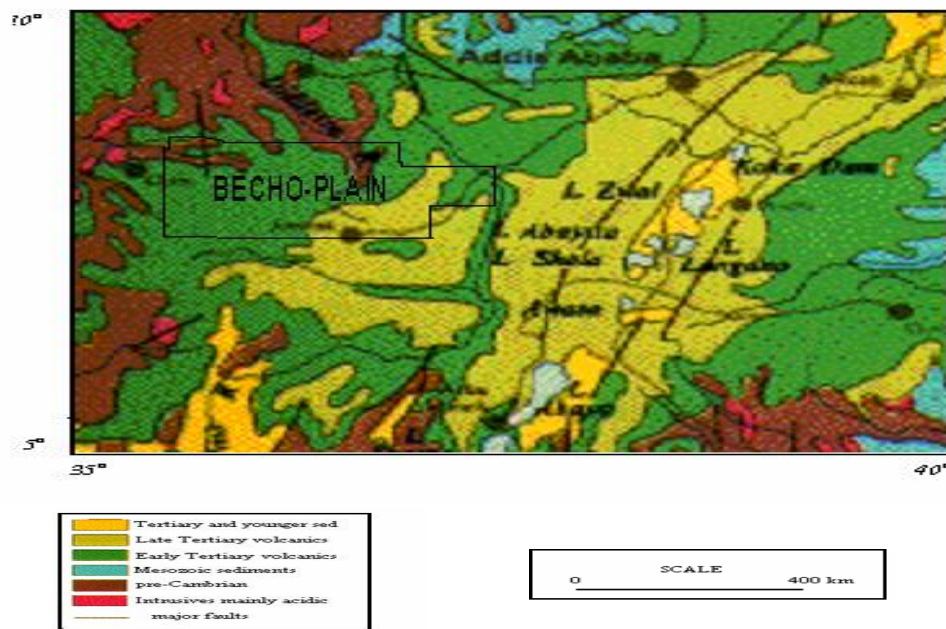


Figure 1.3: Geological map of Becho plain and the surrounding area.

The norher part of the survey area is consisting of rhyolites, ignimbrites and subordinate

trachytes. Obsidian bearing rhyolites are common in the study area. It is grayish to pink brown in colour. The age of this rock unit is Miocene, 33-15Ma (Kazmin, 1979). The quaternary Volcanic rocks outcrop at western and the northern extreme part of the area . It is a lava flow composed of porphyritic basalt with large crystals of plagioclase, olivine and pyroxene, basalt breccias and minor tuff. In the area of Weliso, it is scoriaceous basalt. In the Abay Master plan this unit is mapped as basalt lava flows connected to volcanic center (QVCB) and its age is Pliocene to present.

### **1.2.5 Hydrogeological conditions of Becho plain**

The major task of the hydrological study is to identify the recharge area and quantify the Becho aquifer system. Prior studies have mainly limited the recharge of the area (not specified in the study whether confined or unconfined aquifer) corresponding only to the watershed boundaries of Awash basin, upstream of Awash at Hombele station.

The present hydrological study indicate that deep percolation and transporting mechanism of water from upper Abay and Awash basin to Becho aquifer. The mean annual recharge from the upper Abay basin is  $370\text{Mm}^3$ . The mean annual recharge of the Becho aquifers system is estimated to be  $687\text{Mm}^3$ , with 50% of contributed by Upper Abay basin. Figure 1.4 shows the framework of the Becho plain and the surrounding area.

The following points are considered on the identified recharge area of Becho plain:

- The Becho plain ground water basin is part of the regional ground water and its main recharge area is in Awash river basin (Rift valley) .
- The Becho plain ground water basin is part of the regional ground water and its main recharge area is in Awash river basin (Rift valley) .
- Contiguous highland watersheds of the Abbay basin above the gorges serve as recharge area. Upper watershed of the Muger river (Tributary of Abay river). Aleltu and Robi (tributaries of Jemma river which join Abay river) flowing from Abay Plateau watersheds are major recharging area of the Becho plain ground water basin main confined aquifer.
- The upper watershed of the Awash river above the Becho plain are assumed to contribute recharge in to the upper aquifer of Adaa plain ground water basin.

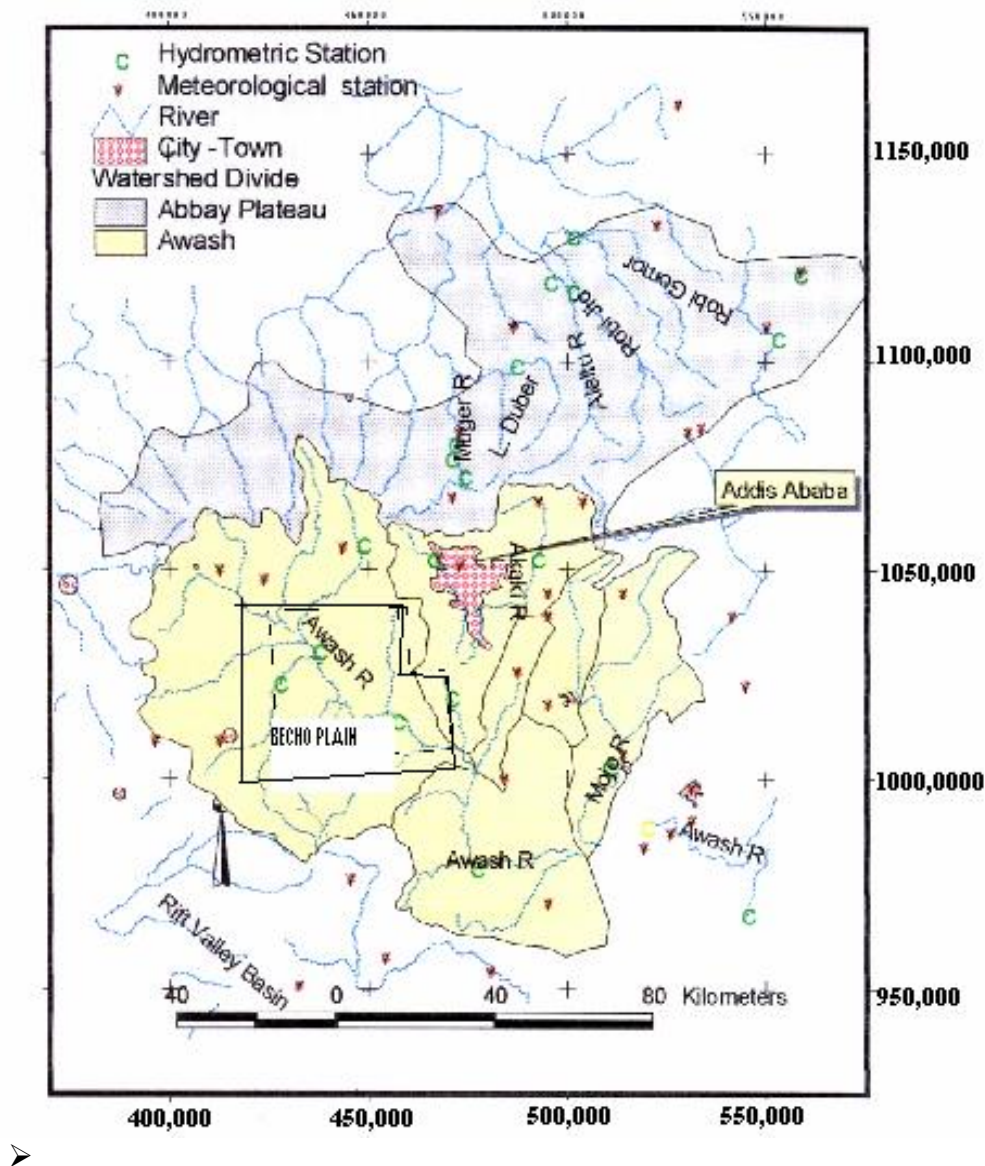


Figure 1.4, The hydrological map of the study area

### 1.3. STATEMENT OF THE PROBLEM AND MAIN OBJECTIVES

#### 1.3.1 Statement of the problems

Ethiopia Ministry of Water Resources commissioned a study on the evaluation and development of Adaa-Becho plain ground water resources for the development of irrigation project commanding more than 2000ha.

Hence, to investigate the area of interest, multi-deciplinary study involving geology, hydrology and geophysics has been undertaken by Water Works Design and Supervision as a consultant. A vast geophysical data of Adaa-Becho plain is now available in Water Works Design and Supervision Enterprise database.

In this thesis work, it is intended to assess the regional ground water condition of Becho-plain using this data. The reason to use the data from this study area is that, geophysical methods may have different possible interpretation based on the method and the approach each interpreter use.

- 

### **1.3.2 Objectives and the scope of the study:**

- to identify major geological structures like faults, lineaments which are important for ground water occurrences, storage and circulations.
- to determine the geophysical response of the different lithological and hydrological units of Becho plain, based on their resistivity contrasts.
- to examine the aquifer properties of Becho plain, including depth to the saturated zones, degree of weathering and fracturing of water bearing formations and thickness and overburden or confining materials.
- To identify the tilt of the fault and the boundary of the aquifer with high yield potential.

# CHAPTER TWO

## 2. THEORETICAL BASIS

### 2.1. THE PRINCIPLE OF GEOELECTRICAL METHODS IN GEOPHYSICAL EXPLORATION.

Theory of electrical prospecting has been developing from the laws governing the behaviors of electrical and electromagnetic fields in a homogeneous conducting earth, (.Zhanov and Keller, 1998)..

The three main groups of electrical exploration methods are natural field electromagnetic methods, controlled source electromagnetic methods (CSEM) and direct current methods (DC). The DC methods include vertical electrical sounding (VES), resistivity profiling, resistivity mapping, and usually the induced polarization (IP methods). The theory for the DC methods is developed under the assumption that constant currents are used, though, in fact, we need to assume that the rate of variation of a current is slow enough that our measurements will be the same as those obtained with the true direct current in the limit. The Max-Well equations, which are a mathematical formulation of the law describing the behavior of electromagnetic fields, are the basis of this theory.

These equations are

$$\nabla \times \vec{E} = -\frac{\partial \vec{B}}{\partial t} \text{-----} 2.1$$

$$\nabla \times H = \vec{j} + \frac{\partial \vec{D}}{\partial t} \text{-----} 2.2$$

$$\nabla \cdot \vec{B} = 0 \text{-----} 2.3$$

$$\nabla \cdot \vec{D} = q \text{-----} 2.4$$

The two forms for electromagnetic field behavior, which are most suitable for use in electrical exploration. These, are the static and quasi-stationary forms.

### 2.1.1 Static electromagnetic fields

Rewriting the equations for static electromagnetic fields and considering the physical phenomenon, we have

$$\nabla \times \vec{H} = \vec{J} \text{-----} 2.5 \qquad \nabla \cdot \vec{B} = 0 \text{-----} 2.7$$

$$\nabla \times \vec{E} = 0 \text{-----} 2.6 \qquad \nabla \cdot \vec{D} = q \text{-----} 2.8$$

The electric field creates conduction currents (sometimes also called galvanic current) which are accompanied by magnetic field, but magnetic field now has appreciable effect on the electric field, if no conduction current (as when the medium is not conducting).

### 2.1.2 Quasi-stationary electromagnetic fields

The quasi-stationary form of electromagnetic field behavior is characteristic of majority technique use in geo- electric exploration; it occurs under conditions in which the components of electromagnetic fields vary slowly enough that the second derivatives with respect to time in the field equation can be ignored.

We have

$$\nabla \times \vec{H} = \sigma \vec{E} \text{-----} 2.9$$

$$\nabla \times \vec{E} = \frac{-\partial \vec{E}}{\partial t} \text{-----} 2.10$$

We don't include divergence and the displacement vector ' $\vec{D}$ ' and permeability ' $\epsilon$ '. So we can conclude that in quasi-stationary regime, electromagnetic fields are independent of the dielectric properties of the medium.

### 2.1.3 Resistivity of rocks

Ohm (1827) described a linear relationship between voltage drop and current flow which usually exists when a material is placed in any electromagnetic field. This empirically observed relationship is universally called Ohm's law, and written as

$$\vec{J} = \sigma \vec{E} \text{-----2.11}$$

The constant proportionality, which arises in ohm's law, is defined as the electrical conductivity of the medium .Because both electric field intensity  $\vec{E}$  and the current density  $\vec{J}$  are a vector quantity. The quantity  $\sigma$  must be a tensor of rank 3, which in Cartesian coordinate will have nine components.

$$\sigma = \begin{vmatrix} \sigma_{xx} & \sigma_{xy} & \sigma_{xz} \\ \sigma_{yx} & \sigma_{yy} & \sigma_{yz} \\ \sigma_{zx} & \sigma_{zy} & \sigma_{zz} \end{vmatrix} \text{-----2.12}$$

The conductivity tensor is symmetric in that the off diagonal terms will have symmetrically equal value  $\sigma_{xy} = \sigma_{yx}$ , and so on. If two of the coordinate directions are selected to lie in the direction of maximum and minimum conductivity tensors ,the non diagonal terms all being zero, leaving only three components along the principal diagonal

$$\sigma = \begin{vmatrix} \sigma_{xx} & 0 & 0 \\ 0 & \sigma_{yy} & 0 \\ 0 & 0 & \sigma_{zz} \end{vmatrix} \text{-----2.13}$$

In isotropic material, the three principal values of conductivity are all the same, and in effect, conductivity is a scalar quantity. In isotropic materials, the electric field vector and current density vector are collinear, current flow along the direction of the applied electric field. In an anisotropic material, defined as one in which the three principal values of the conductivity tensor are not equal .The current density will not flow necessary in the direction of applied electric field . Coincidence of direction occurs only when the electric field is directly along one of the principal direction of the tensor conductivity.

Anisotropy is a common phenomenon in a rocks and minerals .If the dependence of conductivity on a direction exists at a molecular level the isotropy is said to be intrinsic. How

ever aggregated of isotropic minerals in a rock can exhibit a dependence average conductivity on the direction of the applied field, and appear to be anisotropic in bulk .Such behavior is termed as structural anisotropy. In rocks and minerals uniformity in one plane two of the three principal values of the conductivity equal. Almost always, these two equal values are maximum conductivity of material. Such materials are termed gyrotropic.

#### 2.1.4. Dielectric permittivity

Max-well realized the necessary for explaining the transfer of alternating current through the discontinuous circuits, such as capacitors. He described the appearance of opposing charges on the two end of discontinuous circuit as being an electric displacement , measured as a charge accumulation per unit area Q/A. He then postulated a constitute equation relating the amount of displacement to the applied electric force.

$$\vec{D} = \epsilon\vec{E} \text{ ----- 2.14}$$

This equation defines another electric property of a medium,  $\epsilon$ , known as dielectric permittivity. Unlike conductivity, a dielectric permittivity has a well defined values even in the absence of matter, this value is  $8.854 \times 10^{-12}$  farad per meter. In geophysical, IP uses this property.

## 2.2. VERTICAL ELECTRICAL SOUNDING AND APPARENT RESISTIVITY

### 2.2.1 Electrode configurations and geometric factors

Vertical electrical sounding (VES) is perhaps the most commonly used strategy in the application of DC electric methods. It is based on the concept that electrical structure of the earth can be described with one dimensional resistivity function  $\rho(z)$ , with resistivity of a rock varying only with depth with in earth. In fact we would like to believe that lateral change in the resistivity of the earth described by  $\rho(x,y)$  ,is slow that at any point ,the profile  $\rho(z)$  can be determined independently of the lateral variation  $\rho(x,y)$  .Then the lateral change can be determined with a series of vertical electrical soundings made along a profile over an area and interpreted as asset slowly changing  $\rho(z)$  functions.

Alternating current is supplied to the two outer electrodes ,the potential differences across the

inner two being measured by a potentiometer. Since the potentiometer is incorporated in the current electrodes circuit, current through the potentiometer is from the same source as that flowing through the ground. Variation in the supply voltage affects both potentiometer and current electrode equally, therefore does not upset the balance.

Many such standard arrays have been devised over the years, each with some supposed advantage over the others. As the distance between the current electrodes is increased, so the depth to which the current penetrates is increased. In the case of the dipole-dipole separation is obtained by increasing the inter dipole separation not by lengthening the current electrode dipole.

Most of the arrays are based on the use of four electrodes as shown in the Figure 2.1. Two of the electrode contacts, A and B are used to derive current in to the ground, while the other two, M and N, are used to detect the potential drop in the earth.

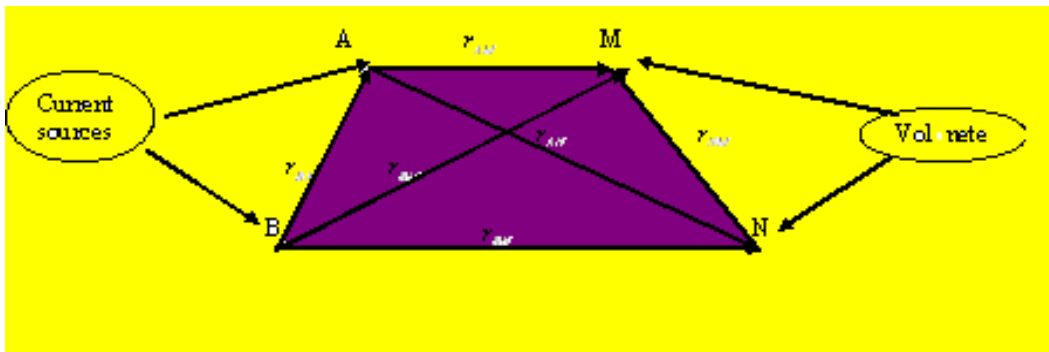


Figure 2.1, plane view of four electrodes.

The four electrodes can be arranged arbitrarily, and apparent resistivity value can be computed, knowing only the electrodes distances, the current and the voltage.

In the analysis of measurements made with such arrays, we will assume that a current  $I$ , injected in to the ground at the point A, and, independently, a current  $-I$  is injected in to the ground at the point B. We measure the voltage  $\Delta U_{MN}$ , at points M and N on the surface of the earth. The voltage according to the Ohm's law, will be proportional to the strength of the

current,  $I$  and depend on the electric properties of earth.

For example in a simple case of homogeneous half space with resistivity ' $\rho$ ', according to the equation which can be derived for appoint source as follow.

The current density at A on the hemispherical surface will be

$$j = \frac{I}{2\pi r^2} \text{-----2.15}$$

using Ohm's law , electric observation at A

can be expressed

$$\vec{E} = \vec{J}\sigma = \frac{\rho I}{2\pi r^2} \frac{\vec{r}}{r} \text{-----2.16}$$

The vector  $\vec{E}$  is directly along the radius vector connecting the point A to M.

Designating the vector A to M at  $\vec{r}$  , the electrical field can be written as

$$\vec{E} = \frac{I\rho}{2\pi r^2} \frac{\vec{r}}{r} \text{-----2.17}$$

where  $\frac{\vec{r}}{r}$  is a radially directed unit vector .

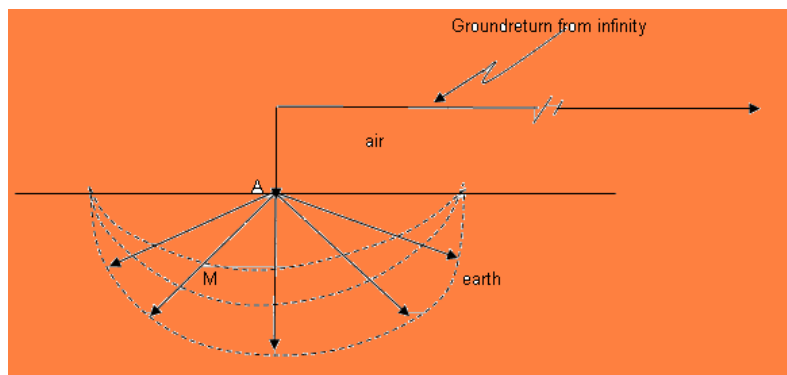


Fig 2.2 A single current source.

Assume origin of the Cartesian coordinate at A and M is designated by coordinate  $M = (x, y, z)$ .

14

The scalar vector length is

$$r = (x^2 + y^2 + z^2)^{1/2} \text{-----} 2.18$$

$$E_x = \frac{I\rho}{2\pi r^2} \frac{x}{r} \text{-----} 2.19$$

$$E_y = \frac{I\rho}{2\pi r^2} \frac{y}{r} \text{-----} 2.20$$

$$E_z = \frac{I\rho}{2\pi r^2} \frac{z}{r} \text{-----} 2.21$$

We should note that vertical component of electrical field is zero at the surface. Physically no current will cross the earth surface to flow in the upper half space, the air.

Since

$$\vec{E} = -\nabla U \text{-----} 2.22$$

Hence

$$U = \frac{I\rho}{2\pi r} \text{-----} 2.23$$

The potential at the point M will be the sum of contribution from the current flowing through the point contact A and B as follows.

$$U_M = \frac{I\rho}{2\pi} \left\{ \frac{1}{r_{AM}} + \frac{1}{r_{BM}} \right\} \text{-----} 2.24$$

and similarly for the potential at the point N

$$U_N = \frac{I\rho}{2\pi} \left\{ \frac{1}{r_{AN}} + \frac{1}{r_{BN}} \right\} \text{-----} 2.25$$

Where the distances  $r_{AM}, r_{BM}, r_{AN}, r_{BN}$  are defined as shown in the *Figure 2.1*.

Consequently,

$$\Delta U_{MN} = U_M - U_N \text{-----} 2.26$$

$$= \frac{I\rho}{2\pi r} \left\{ \frac{1}{r_{AM}} - \frac{1}{r_{BM}} + \frac{1}{r_{BN}} - \frac{1}{r_{AN}} \right\} \text{-----} 2.27$$

In this model,  $\nabla U_{MN}$  is proportional to the resistivity, ‘ $\rho$ ’.

$$\rho = \frac{2\pi\Delta U_{MN}/I}{\left\{ \frac{1}{r_{AM}} - \frac{1}{r_{BM}} + \frac{1}{r_{BN}} - \frac{1}{r_{AN}} \right\}} \text{-----} 2.28$$

$$K_g = \frac{2\pi}{\left\{ \frac{1}{r_{AM}} - \frac{1}{r_{BM}} + \frac{1}{r_{BN}} - \frac{1}{r_{AN}} \right\}} \text{-----} 2.29$$

$$= K_g \frac{\Delta U_{MN}}{I} \text{-----} 2.30$$

where ‘ $K_g$ ’ is the geometrical factor for the array of electrodes being used to measure resistivity. The ratio  $\frac{\Delta U_{MN}}{I_{AB}}$  is called the mutual resistance ‘ $R_m$ ’ and is measured in Ohms.

The final expression of the equ (2.30) has two parts, namely a resistance term (R; unites $\Omega$ ) and a term that describe a geometry of electrode configuration which is known as the geometrical factor (K; unites m). In reality, the subsurface ground does not conform to a homogeneous medium and thus the resistivity obtained is no longer the ‘true’ resistivity but the apparent resistivity ( $\rho_a$ ) which even can be negative. It is very important to remember that the apparent

resistivity is not a physical property of the sub surface media,unlike the true resistivity. Consequently,all field resistivity data are apparent resistivity while those obtained by interpretation techniques ‘true’ resistivities.In order to get at least 50% of the current to flow through an interface at adepth of z metres in to asecond medium,current electrode separation needs to be at least twice-and preferably more than three times-depth.This has obvious practical implications ,particularly when dealing with a situations where the depths are the order of several hundreds of meters,so require very long cable lengths that can produce undesirable inductive coupling effects.For very deep soundings where the electrode separation is more than several kilometers,telemetering the data becomes the only practical solution(eg Shabtaie et al.1980,1982).However.it should be emphasized that it is misleading to equate the depth of penetration with the current electrode separationas a general rule in the region of resistivity survey.

Mutual resistance is not a resistance in ordinary sense in as much as the voltage and current are measured in separate circuits. For the mutual resistance to be meaningful, the two circuits must be linearly coupled so that the ratio is constant.

The most commonly used standard electrode array for sounding is the schlumberger array with four electrodes symmetrically located about the mid point of the array, and with inner two electrodes M and N being closely spaced so that in effect.The component of electrical field along the array axis is measured .the outer electrodes ‘A’and ‘B’are used to inject current in to the earth .

For schlumberger array,  $r_{AN} = r_{BM}$  ;  $r_{AM} = r_{BN}$  and the equation (2.29) provides the following values for the geometrical factor

$$K_g = \frac{\pi r_{AN} r_{AM}}{r_{AN} - r_{AM}} \text{-----} 2.31$$

$$r_{AN} = s + \frac{b}{2} \text{-----} 2.32$$

$$r_{AM} = s - \frac{b}{2} \text{-----} 2.33$$

$$s = \frac{r_{AB}}{2} \text{-----2.34}$$

Often, it can be assumed that

$$K_{\text{gschlumberger}} = \frac{\pi \left[ s^2 - \frac{b^2}{4} \right]}{b} \text{-----2.35}$$

$$= \pi \frac{s^2 \left[ 1 - \left( \frac{b}{2s} \right)^2 \right]}{b} \text{-----2.36}$$

Outer spacing  $s = \frac{r_{AB}}{2}$

Inner spacing  $b = r_{MN}$

so that

$$\left( \frac{b}{2s} \right)^2 \ll 1 \text{-----2.37}$$

$$K'_{\text{gschlumberger}} = \pi \frac{s^2}{b} \text{-----2.38}$$

So that equation can be simplified to

$$\rho_a = \pi \frac{s^2}{b} \frac{\Delta U_{MN}}{I} \text{-----2.39}$$

The first geometric factor is exact with no approximation being made, while the second is based on approximation that the inner spacing is small enough that the term  $\left( \frac{b}{s} \right)^2$  can be ignored in comparison with unity. It is quite reasonable that we should be able to determine

resistivity of a homogeneous half space in this simple way.

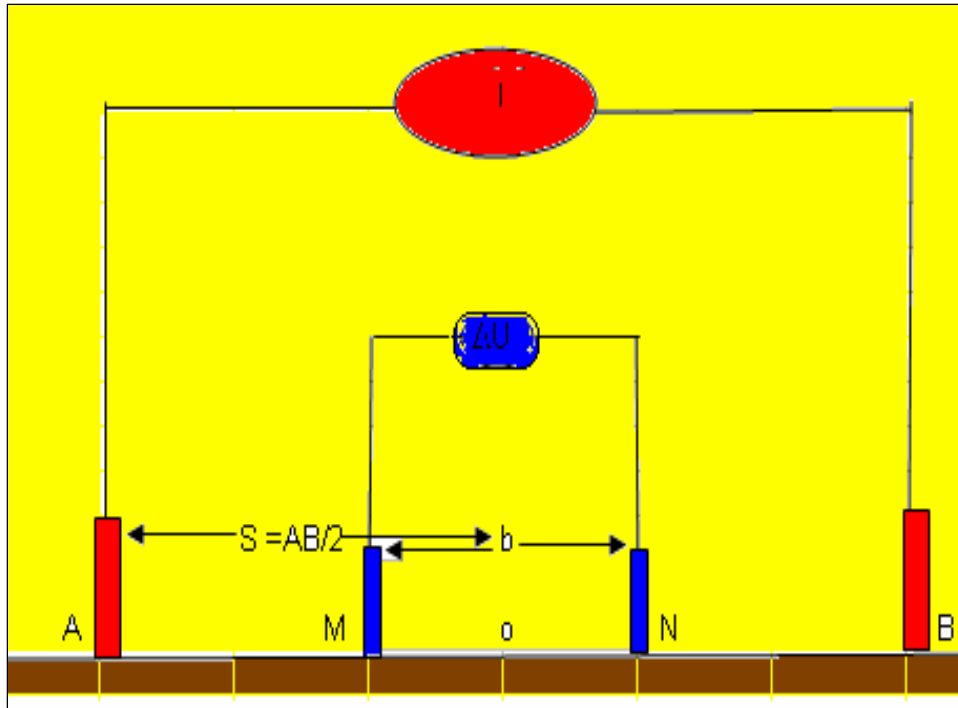


Figure 2.3, four electrodes linear array for Schlumberger .

By increasing the separation between the current electrodes in schlumberger array, we can effectively increase depth to which we can sense resistivity in the earth. This concept involves in geometrical sounding.

It should be avoided creating the impression that the depth of investigation is related solely to the separation between electrodes. It is important to know the theory of reciprocity .This theorem is absolutely valied . It states that if the role of the two current electrodes ‘A’ and ‘B’ are interchanged with the roles played by measuring electrodes ‘M’ and ‘N’, there would be no change in measured quantities, current and voltage. No matter what geoelectrical structure of the earth is. The depth of investigation a chieved in geoelectrical sounding is related to many things and not merely the geometry of sounding. Writing the expression for the apparent resistivity measured with an ideal schlumberger array in which the approximation

$$E = \frac{\Delta U_{MN}}{b} \text{ is valid provide that the result.}$$

How ever if the distance  $r_{MN}$  is made small enough, the ratio  $\frac{\Delta U_{MN}}{r_{MN}}$  comes close to the value of  $E_{MN}$ , the component of electrical field along the line connecting the electrodes ‘M’ and ‘N’. We often claim to use these ratios to measure the electrical field component at O, half between ‘M’ and ‘N’. However this is only an approximation and in field practice it is seen that the limiting processes not well observed and the measured electric field component can be poor estimate of mathematical electric field.

This is

$$E_{MN} \approx \frac{\Delta U_{MN}}{r_{MN}} = \frac{\rho I}{2\pi r_{MN}} \int_0^\infty \left[ \frac{1}{r_{AM}} - \frac{1}{r_{BM}} + \frac{1}{r_{BN}} - \frac{1}{r_{AN}} \right] \dots\dots\dots 2.40$$

$$\rho \approx \frac{2\pi r_{MN} E_{MN} / I}{\left\{ \frac{1}{r_{AM}} - \frac{1}{r_{BM}} + \frac{1}{r_{BN}} - \frac{1}{r_{AN}} \right\}} \dots\dots\dots 2.41$$

Some times the significant error in comparing measured electric field with computed electric fields for some model are being tested interpretation. The measured electrical field for a general four-electrode array and a homogenous earth with resistivity  $\rho$  is given by (2.41) and the inversion of this expression to obtain a solution for resistivity in terms of measured quantities fields. In the real world, the only characteristic of the field we can measure is voltage drop between two electrode contacts .The potential and electric field are idealized mathematical concepts not exactly measurable

$$K_g^E > Z_m \dots\dots\dots .42$$

$$K_g^E = \frac{2\pi r_{MN}}{\left\{ \frac{1}{r_{AM}} - \frac{1}{r_{BM}} + \frac{1}{r_{BN}} - \frac{1}{r_{AN}} \right\}} \dots\dots\dots 2.43$$

Where  $Z_m = E_{MN}/I$  mutual impedance and  $K_g$  is the geometric factor for use with electric field measurements.

Writing an expression for the apparent resistivity measured with an ideal Schlumberger array in which

$$E_r \approx \frac{\Delta U_{MN}}{b} \text{-----2.44}$$

the approximation that is valid .

$$\rho = K_g \frac{\Delta U_{MN}}{I} \text{-----2.45}$$

Steafanescue's (1930) equation of electrical potential,  $U(r)$  on the surface of the layered earth at distance  $r$  from a point source of strength 'I' is written as

$$U(r) = \frac{I}{2\pi} \int_0^{\infty} T(\lambda) J_0(\lambda r) d\lambda \text{-----2.46}$$

where  $J_0(\lambda r)$  is the Bessel function of first kind and zeroeth order,  $T(\lambda)$  is the resistivity transformation function at air-earth interface, and  $\lambda$  is the integration variable.

Sri Niwas and Is rail (1986) used an exponential approximation of  $T(\lambda)$ , as

$$T(\lambda) = \sum_{j=0}^{\infty} c_j e^{-\xi_j \lambda} \text{-----2.47}$$

where  $c_j$  is the coefficient of  $j$ -th approximating function and  $\xi_j$  establishes the position of approximating function along the abscissa, to reduce the integration equation (2.40) through Lipschitz integral to a simple algebraic equation making numerical computation easy once the  $C_j$  and  $\xi_j$  are estimated.

### 2.2.1 Transformation of Wenner to Schlumberger apparent resistivity over layered earth

Of the two main field techniques which are used in resistivity sounding, the Schlumberger method is superior to the Wenner is that the field applications are easier and there is lesser influence of lateral inhomogeneities in the measurements (Kunetz, 1966; Keller and Frischknecht, 1966; Ehattacharya and Patra, 1968).

The Wenner method, however, may have some advantages under certain field conditions in that the Wenner potential measurements are more stable than the potential gradient measurement of the Schlumberger system with the same quality of measuring equipment (Kunetz 1966). Unlike the Schlumberger system the number of available tools for interpreting the Wenner data is meagre as the master curves for this system are very few (Orellana and Mooney, 1966) and the handy auxiliary point method (Zohdy 1965) could not be used in its present form.

Thus the idea of transforming the measurements and interpreting it in the Schlumberger domain with better know how and abundant interpretational techniques would be useful. Deppermann (1954) studied the interrelationship between the two systems and developed a numerical scheme to transform Wenner curves to Schlumberger curves.

Where  $s = r_{AO}$  ,

$$E_r = \frac{-\partial U}{\partial r} \approx \frac{\Delta U}{b} = \frac{I}{2\pi} \int T(\lambda) \frac{\partial J_o(\lambda r)}{\partial r} d\lambda \quad \text{--- 2.48}$$

$$\frac{\partial J_o(\lambda r)}{\partial r} = -J_1(\lambda r)\lambda \quad \text{----- 2.49}$$

$$\rho_{as} = K_{gschl} \frac{\Delta U}{I} = \pi \frac{s^2}{b} \frac{\Delta U}{I} = \pi \frac{s^2}{I} \frac{\Delta U}{b} \quad \text{--- 2.50}$$

$$E_r = \frac{I}{2\pi} \int T(\lambda r)(-J_1(\lambda r))\lambda dr \quad \text{----- 2.51}$$

$$= \pi \frac{s^2}{I} \frac{I}{2\pi} \int T(\lambda r)(-J_1(\lambda r))\lambda dr \quad \text{----- 2.52}$$

$$= \frac{s^2}{2} \int T(\lambda r)(-J_1(\lambda r))\lambda dr \quad \text{----- 2.53}$$

Compare (2.52) and (2.54)

$$\rho_{aw} = K_g \frac{\Delta U}{I} = 2\pi \frac{a}{I} \int T(\lambda r) (-J_1(\lambda r)) \lambda dr \text{-----} 2.54$$

$$= a \int T(\lambda r) (-J_1(\lambda r)) \lambda dr \text{-----} 2.55$$

$$\frac{2\rho_{as}}{s^2} = \frac{\rho_{aw}}{a} = \int T(\lambda r) (-J_1(\lambda r)) \lambda dr \text{-----} 2.56$$

When  $\rho_{as} = \rho_{aw} \Leftrightarrow s = \sqrt{2a}$  Where  $s = r_{AO}$ . This suggests that the schlumberger collection of standard graphs may be used for curve matching the wenner data if one puts the cross at  $s=1.4$  and  $\rho_a=1$ . This popular but approximate method was used by geophysicists to interpret the wenner data until Orellena and Mooney supplemented their original 1966 collection with a wenner set. In recent years, the linear filter method has been used to interpret the Schlumberger and Wenner soundings independently (Ghosh 1970, 1971a, b). Filters were developed to convert the apparent resistivity to the kernel and vice-versa.

An additional but easily resolvable problem can occur with Schlumberger depth soundings. When the separation of the potential electrode pair is increased, the contact resistance may change, causing a discrete set up or down of the next segment of the curve.

Although the value of the apparent resistivity may change from the use of one electrode pair to another, the gradient of the change of apparent resistivity as a function of current electrode half space separation should remain the same. Consequently, the displaced segments can be restored to their correct values and the curve smoothed ready for interpretation. Segments at larger potential electrode separation should be moved<sup>23</sup> to fit the previous segment obtained with a shorter electrode separation.

Measurements of resistance should be repeated at both potential electrode separations when crossing from one segment to the next.

### 2.2.2 Comparison of Dipole-dipole, Schlumberger, Square and Wenner electrode arrays

Criteria	Wenner	Schlumberger	Dipole-dipole	Square
Vertical resolution	g	m	p	m
Depth penetration	p	m	g	m
Suitability to VES	m	g	p	u
Suitability to CST	g	u		g
Sensitivity to orientation	y	y	m	n
Sensitivity to lateral inhomogeneities	g	m	m	l
Labour intensive	y(n*)	m(n*)	m (n*)	y
Availability of interpretational aids	g	g	m	p

p=poor,m=moderate,g=good,u= unsuitable;y=yes;n=no;h=high;l=low

\* when using a multicore cable and automated array

Table 2.1 The comparison between Dipole-dipole, Schlumberger, Square and Wenner according to the criteria listed ( JohnM.Rnolds).

### 2.2.3 Schematic presentation of eight electrode configurations considered

Figure 2.4 shows the different possible orientation of four electrode arrays .Generally they are eight in number. They have their own advantage and disadvantage. It is discussed in detail (.Zhdaov and .Keller).

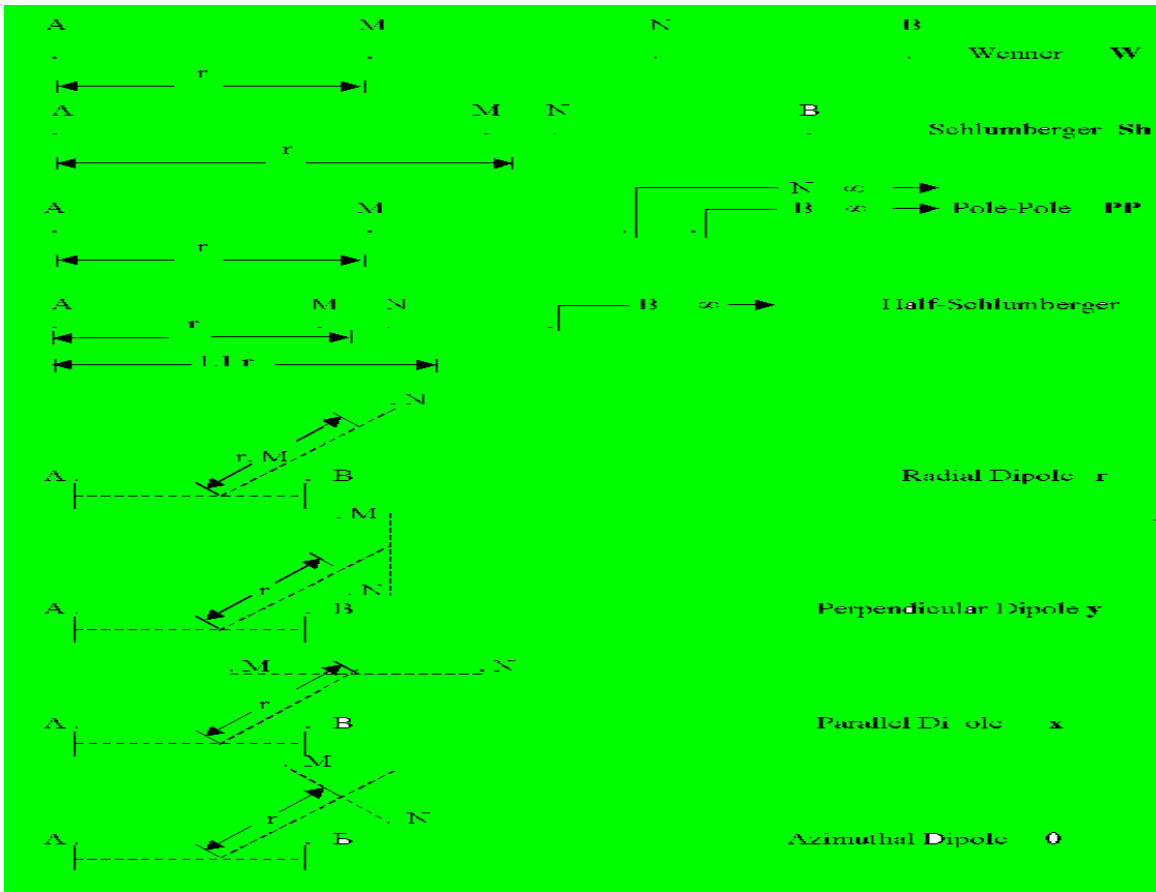


Figure 2.4, the eight electrode configurations

### 2.3 TIME DOMAIN ELECTROMAGNETIC SOUNDING

Beginning in the 1960s, interest developed in the use of controlled source electromagnetic sounding to explore to the depth of importance in exploration for oil, direct gas and for geothermal system.

In a typical TDEM survey, a large current is passed through a large un grounded loop transmitter to energized it . After a discrete period of time (a few tens of milliseconds ) ,during which any effect due to the switching the current on would have died away ( known as ‘ turn-on transient’ ) . The applied current is interrupted abruptly .If the conductor is present with in the vicinity. The sharp change in the primarily field will induce eddy currents with in the conductor initially at it surface only .

This is known as the ‘early - time’ stage’ of the transient process. These surface currents then start dissipating through ohmic losses .The zone immediately with in the conductor then

experiences a decreasing magnetic field with a consequential flow of eddy currents through it. Effectively this is the start of the inward diffusion of the current pattern caused by the eddy currents towards the interior of the conductor. This is the 'intermediate-time stage' of the transient process.

The final or the 'late -time stage' of this process is reached when the induced current distribution is invariant with time. The only change observed is a decrease in the over all amplitude with time. If the conductor present is very large relative to the dipole source being used , the eddy current may be spread out laterally as well as diffused in to the interior of the conductor .The rate of change of these currents and of their respective magnetic field depends on the size and shape of the conductor and on its conductivity . In contrast the initial distribution of the surface current is dependent only on the size and the shape of the conductor as this is geometrical phenomenon, not one due to the conductivity of the body.

The whole process of the step-wise excitation of the current loop is repeated many times and the data stacked for a given location. The transient electric field reaches maximum at a distance known as the diffusion depth (d) which is for TEM what the skin depth  $\delta$  is to frequency -domain EM. In the time domain diffusion depth is directly proportional to  $\sqrt{t}$  , where as in frequency domain it is inversely proportional to  $\sqrt{\omega}$  (where  $\omega = 2\pi f$ ) .This local maximum propagates down wards with a finite velocity (v).

In the case of a semi-infinite half space, i.e. uniform horizontally layered media, the 'early -stage' surface currents are located primarily in the vicinity of transmitter loop, much like the down ward movement of a system of smoke rings Fig[2.6] with a consequential decay of the amplitude with time .The same principle applies in the case of a horizontally layered earth. Normally the ground materials are assumed to be non- polarisable and conductivity is taken to be independent of frequency or delay time.

These induced polarisation effects affect the reliability of interpretation. Where materials with in the ground have slight variations in magnetic permeability, typical of the order of 1% of the earth magnetic field intensity (e.g.550nT in a field of 55000nT) small TEM effects may be detectable. The TEM response is likely to be enhanced by about 1% in such cases.

Where lateritic soils are present, super paramagnetic effect may cause anomalous transient recording with the SIROTEM system. It manifests as  $1/t$  dependence which results in erroneous determinations apparent resistivity with time. Similar effects are also likely to occur where either conductivity or magnetic permeability of the ground varies as a function of frequency. Removal of super paramagnetic effects can be achieved by displacing the receiver loop by 2-3m relative to the transmitting loop where deployed in coincident loop configuration.

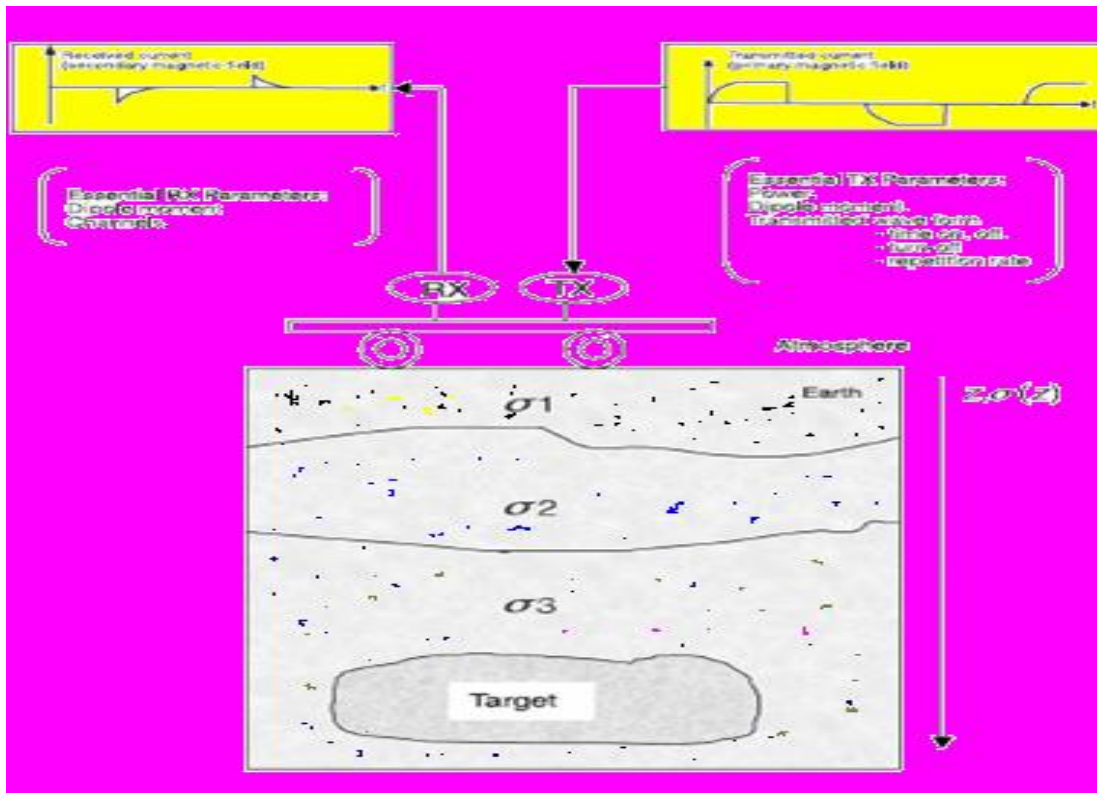


Figure 2.5 The time-domain EM wave forms.

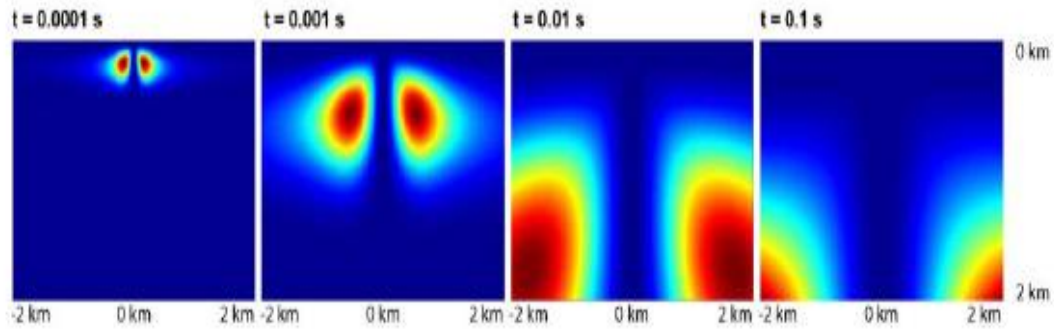


Figure 2.6, the form of eddy current that propagates down ward and out ward like smoke rings at successive interval of time.

### 2.3.1 Sources of error in TEM measurements

There are three principal sources of *error* in TEM measurements:-

- (a) Geometrical errors in transmitter receiver positions and topographical effects
- (b) Static cultural noise; (c) Dynamic cultural noise.

Most TEM methods are largely insensitive to geometrical errors and in the case of a resistive ground are relatively insensitive to topographic effects. However a conductive overburden is present topography can produce severe coupling errors and deliberate procedure need to be followed to correct for such effects (Nabighian and Macnae 1991)

Static cultural noise arises from the presence of the pipes and cables, metal fences or other utilities present in the survey area .Some metallic utilities serve as current channellers which causes distortions in TEM data. Live electric cables have distinctive effects at a particular frequencies and their harmonics but these can be readily removed by notch filtering(band stop filter) .The effect of channeling can be reduced by laying the transmitter loop symmetrically over the utility.

Dynamic cultural noise is caused by a number of sources .At frequencies less than 1Hz, the source is geomagnetic signals from within and above the earth's ionosphere. At frequencies above 1Hz, typically in the 6-10 Hz range, signal generated by distant lightning discharges

produces sferics which are natural EM transients. Higher frequency sources of noise are a.c. power (50-60Hz) and VLF transmitter (10-25 KHz). Of particular importance in airborne EM and in surveys undertaken in a wide open space is wind noise which causes motion of magnetic field sensors within earth's magnetic field. The fields used in TEM work are typically five orders of magnitude smaller than the earth's magnetic fields. In uniform conducting medium, transient electric field achieves a maximum at the diffusion depth (d) such that :

$$z = (2t/\sigma\mu)^{1/2} = d \quad \text{where } \sigma \text{ and } \mu \text{ are conductivity and magnetic permeability of the medium.}$$

The maximum travels downwards with a velocity (v) such that:

$$v = (2\sigma\mu t)^{-1/2}$$

Electromotive force induced in the earth and near by target by the rapid transmitter current turn-off, secondary magnetic field resulting from eddy current flow in the earth and near by target.

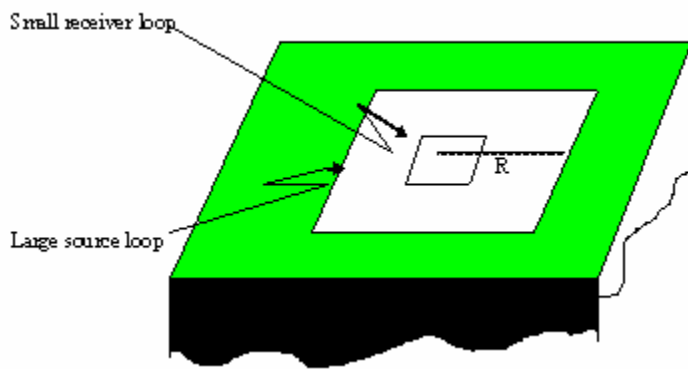


Figure 2.7 Central loop induction method for carrying out Time-Domain electromagnetic soundings . The large loop is energized with a square-wave current. The receiver is sensitive magnetometer is placed at the center of source loop.

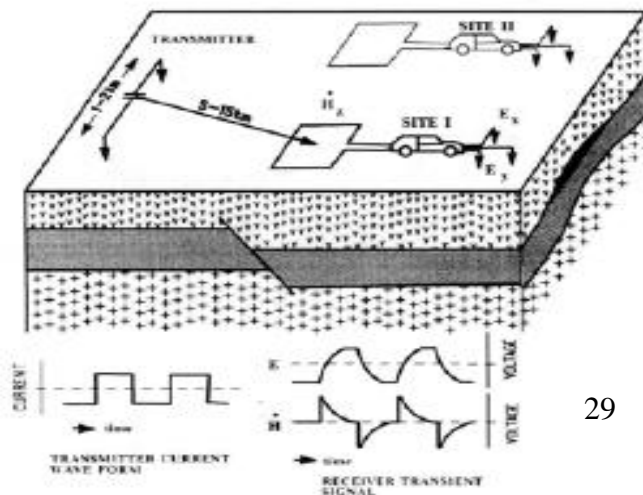


Fig 2. Grounded wire source method for carrying out Time-Domain electromagnetic soundings. The sounding source is energized with a square-wave current .The receiver is a sensitive magnetometer, shown here as a vertical axis loop.

Two nearly equivalent lay outs for doing Time-Domain electromagnetic soundings are shown above. TDEM sounding can be carried out with a variety of sources and receivers. But by far the greatest amount of use has been based on the coupling between a short grounded wire and a sensor that detects the time rate of change of the vertical component of magnetic field from the square wave energized sources or the coupling between two concentric un grounded loops. These are analytically identical systems but do differ to the same extent in operating characteristics. The two arrays are shown in the fig[2.7] and[2.8] .

The conversion of observed data to the values of apparent resistivity is to be desired but with controlled source electromagnetic methods. The definition of apparent resistivity is neither standard nor obvious.

The concept of early and late apparent resistivity for the TDEM method were first proposed by Keller (1969) and by Kaufman and morozova ( 1970) for the most commonly system for the time-domain electromagnetic sounding. One in which an electromagnetic field generated using a current dipole source and the vertical component of the magnetic field is observed . If the system is deployed on the surface of a uniform-half space, the vertical component of magnetic field is:

$$\frac{\partial H_z}{\partial t} = \frac{3Idl \sin \phi}{2\pi\sigma\mu_0 R^4} \left\{ \Phi(u_t) - \left(\frac{2}{\pi}\right)^{\frac{1}{2}} e^{-u_t^2} u_t \left(1 + \frac{u_t^2}{3}\right) \right\} \text{----- 2.56}$$

where  $u_t = \frac{2\pi R}{T_t}$  and  $T_t = 2\pi \sqrt{\frac{2t\rho}{\mu_0}}$

R is the separation between source and the receiver , I is the amplitude of the current step supplied to the source dipole( Idl M is the moment of the source ), t is the time following initiation of the heaviside step , and  $\phi$  is the angle defined in.

The  $\Phi(u_t)$  is the error function .Apparent resistivity is a useful concept .It permits the conversion of field observations to a numerical estimate earth resistivity which can then be used as a guide to the meaning of the measurements made in the field.

With the controlled-source electromagnetic methods ,a more limited form of apparent resistivity can be used for the same purpose by taking only limiting values for the field at very short and very long times.

For example , if one takes a limit for the expression above for a very short times , then

$$\frac{\partial B_z}{\partial t} = \frac{3\rho_t Idl \sin \phi}{2\pi R^4} \text{-----2.57}$$

where  $B_z = \mu_o H_z$

This expression for early time is algebraically simple and can be easily be inverted to find where it has been assumed that the field is detecting using a vertical axis coil with an area  $A_r$  with  $n_r$  turns producing a voltage out put  $V_{coil}(t)$ .

$$\rho_{a,early} = \frac{2\pi R^4}{3A_r n_r Idl \sin \phi} V_{coil} \text{-----2.58}$$

It must be observed that it is meaningful only for the very early portion of a recorded transient. A limit can be taken for the expression in the equa(2.56) for the condition  $t \rightarrow \infty$  as well;

$$\frac{\partial B_z}{\partial t} = \left( \frac{\mu_o^{5/2} NR \sin \phi}{40\pi^{3/2} t^{5/2} \rho^{3/2}} \right) \text{-----2.59}$$

Similarly,this can be solved easily for a definition of apparent resistivity for late time.

$$\rho_{a,late} = \left[ \frac{\mu_o^{5/2} A_r n_r MR \sin \phi}{40\pi^{3/2} t^{5/2} V_{coil}} \right]^{2/3} \text{-----2.60}$$

Both resistivity of the half space and transmitter-receiver separation determine the earliest time at which this late-time definition of apparent resistivity is reasonably valid.

On the examining of these two definition of apparent resistivity equ(2.58) valid for early time (or short separation) and equ(2.60) for the late time(or for long separation).

### **2.3.2 Ground water exploration**

The development during the 1980s of TEM systems with faster shut off rates and earlier time sampling resulted in an increase use of TEM in hydrogeology. Time domain EM exploration is widely used in the search for groundwater.

A theoretical approach has been described Fitterman and Stewart (1986) which provides a range of hypothetical TEM responses for arange of commonly found hydrogeological problem.. You can get real time-domain EM data from South California and transient have been coverted to apparent resistivity Taylor et al., (1992).

Note that the high resistivities at early times are an artefact of using the later time approximation to compute apparent resistivity.

### 2.3.3 The comparison between TEM and VES

	Advantages	Disadvantage
VES	<ul style="list-style-type: none"> <li>-sensitive to both resistivity and conductivity</li> <li>-the data depends on the orientation of the bipoles with respect to the strike of underlying geology or superficial topography</li> </ul>	<ul style="list-style-type: none"> <li>- for thin layer ,problem of nonuniqueness or equivalence become severe</li> <li>-less sensitive to layers with high resistivity</li> <li>-the uncertainty in VES data arise from vertical shifts between apparent resistivity segments.</li> </ul>
TEM	<ul style="list-style-type: none"> <li>-Higher resolving power</li> <li>-Higher quality</li> <li>-Higher data redundancy,</li> <li>-Better data quality</li> <li>-Less sensitivity to topographic and near-surface inhomogeneities and less to equivalence problems associative thin conductive layers</li> <li>-more efficient field operation both in time and physical effort</li> <li>-smoother observed curves</li> <li>-Less sensitivity to perturbing effect associated</li> <li>-small size</li> </ul>	<ul style="list-style-type: none"> <li>-data errors in The TEM sounding arise from electromagnetic noise produced by thunder storm</li> <li>Unlike early time, late time has large error,</li> </ul>

Table 2.2 The comparison between the advantage and the disadvantage of TEM andVES.

## **CHAPTER THREE**

### **3. GEOPHYSICAL SURVEY AT BECHO-PLAIN**

#### **3.1 VERTICAL ELECTRICAL SOUNDING**

##### **3.1.1 Source Data**

Thirty one vertical electrical sounding data, used for this thesis work, were obtained from Water Works Design and Supervision Enterprise. Since the primary aim of geophysical survey is to confirm an inferred ground water barrier and to map the hydro-stratigraphy of the study area, the sounding were conducted in the vicinity of anticipated subsurface divided, and along the two major zones where deep and shallow water level are thought to be encountered .

Generally, the resistivity survey were not conducted on a regular grid thus, the spacing of the VES points were not uniform. They are rather dictated by geology, topography and accessibility of the area under investigation. The symmetrical Schlumberger electrode separation,  $AB/2= 1000\text{m}$ , was chosen based on the depth of interest, (the anticipated depth to the water bearing horizon and subsurface geology).

During data acquisition, the apparent resistivity versus half current electrodes separation were plotted on log-log paper right in the field, as a measure quality control. If any error is detected during the data acquisition, it was automatically corrected either by taking repeated measurements or by improving the contact resistance of the electrode or by changing the position of the measuring electrodes.

##### **3.1.2 Instrumentation**

The instruments used by WWDSE, for electrical soundings resistivity (VES) survey, were portable integrated resistivity meters, Terrameter, SAS 1000A and OYO MC OHM.Mark-2,model 2115A and the maximum current electrode separation  $AB/2$  was 1000 meters.

### **3.1.3 Data processing and presentation of resistivity survey**

The raw data were used to construct various plan maps at different pseudo-depths. These planar maps were later stacked as depth section to depicted both lateral and vertical variations at regional scale. Moreover, the lateral image plot at 750m depth is presented for discussions of geoelectrical parameters at deeper horizon. All qualitative presentations discussed above were handled by mapping softwares such as *Surfer 8 and CoreDraw-10*.

VES field curves along two representative profiles are interpreted, quantitatively, using computer assisted modeling and inversion, *WinResist*. VES field data may have subtle inflections and cusps that require the interpreter to make decisions as to how deal with such features. To over come these problems, noisy field curve were smoothed to produce more suave graphs which can then be modeled more easily. In addition to this, some points which deviates erratically from the synthetic curves are masked to minimize the root mean square (RMS) errors. As a rule, RMS errors, between the theoretical curve and field data, less than 5% are accepted. Furthermore, near- surface layers tend to be modeled more accurately than those at depth. This is primarily because field data from shorter electrode separation are better resolved, owing to higher signal - to- noise ratios.

Each VES data, along the two profile line, was inverted by using the above software. From these inversions, depths (thickness) and resistivities were determined. These values were then used to construct three 1-D geoelectrical sections and four 3-D geoelectrical sections. That is for 2-D geoelectrical section  $\rho(x, z)$  and for 3-D  $\rho(x, y, z)$ . For 1-D geoelectrical section for VES *Figure 4.3-4.5*, for TEM, *Figure A.3.1*, for 2-D geoelectrical section, for 3-D *figure A.2.1- A.2.4* are plotted.

## **3.2 TRANSIENT ELECTROMAGNETIC METHOD (TEM)**

### **3.2.1 Data acquisition of Transient Electromagnetic Method (TEM)**

The TEM data is acquired using PROTEM47 and PROTEM 57 transmitter and PROTEM D

receiver, (GEONICS). The transmitter is set at the edge of transmitter loop which is  $200m \times 200m$  and  $400m \times 400m$  size and attached to Honda generator and transmitter about 10Amp with  $400m \times 400m$  loop size and about 20Amp for  $200m \times 200m$  loop size .The receiver works with seven Repetition Rate(RR). They are marked as u,v,H,M,L,K, and J which represent 237.5 ,62.5 ,25 ,6.25, 2.5, 0.625 and 0.25Hz.

After set up the instrument, three sweeps were collected for TEM57 transmitter, which are H,M and L sweeps and data are acquired in the receiver. All function are controlled by an internal computer which receives instructions from the operator via a pair of key pads and Prompts the message or displays the result on the character/graphic liquid display panel.Also ,Operation of the receiver is fully menu deriven.More over,collected data is dumped in to the field laptop computer through RS232 cable.The data is then checked using the TEM21XID software and the selcted sweep was checked.

Transient electromagnetic TEM PROTEM-%&MK2 instrument. Transient Electromagnetic Method (TEM) survey was conducted at the well sites and selected places at Becho plain to complement the previous done Vertical Electrical Sounding(VES) survey.

### **3.2.2 Data processing and presentation of TEM surveys**

For this study , one TEM sounding was used which was done in study area.Its position is almost in central zone .This TEM sounding data was already processed . Its data inverted value for depth (thickness) and resistivity values was used to construct joint geoelectrical section with VESB16 and VESB17.

Since there are many ways in which TEM data can be processed and these are largely dependent up on which instrument system is used to acquire the original data . Most TEM system record the transient voltage at a number of discrete intervals during the voltage decay after the applied current is swich off.Each time the currnt is applied and then stopped. Measurements are taken. When the current is applied again (swich on) and swich off.

A repeated set of measurements is taken.This process may be repeated many times at a given location with all data being logged authomatically.Consequently these data can be processed

to improve the signal-to-noise ratio .At the same time the field data are checked for repeatability .

Commonly the data are normalized with respect to transmitter current or other system parameter and effect of the same decay may be applied in compensation by normalizing the observed field at each point with respective primary field value at the same point. As the field measuring system become more sophisticated and the amount of data increases. More careful thought needs to be given to the often quite involved data processing sequences now available. For example Stephanetal.(1991) describe a data processing sequence for 'long offset transient'(LOTEM) sounding undertaken in Germany .

These data processing stages were formulated: (a) prestack processing (b) selective stacking processing and (c) post-stack processing. Prestack processing was used to remove unwanted periodic noise using filtering such as notch filter to remove the noise associated with a.c. power lines and Germany electrical railway grid .

A selective stacking algorithm was applied to average only a percentage of the data around the median of the individual time samples. The consequence of this was to reduce the noise content by improving the signal - to-noise ratio .

The final stage was to apply a slight time variable smoothing filter. The culmination of this process was the production of logarithmic plots of a apparent resistivity as a function of decay time . A variety of plots of processed data can be produced such as transient decay (logarithmic) plots of voltage (in mV) versus decay time (in milliseconds) response profile (graphs of measured voltage at selected decay time at all station in a survey area).

Interpretation methods are as varied as the different types of data plots and system used to acquire data . The first is to locate a possible sub surface target on the basis of the shape size and location of anomalies evident on the profiles and maps of relevant parameters .

The second and more quantitative stage is to determine the 'quality' of the conductor using time constants determined from decay plots of the field intensity at one or more locations. Various types of display parameter are useful for different applications. For example ,apparent resistivity sounding can be extremely useful in hydrogeological investigations and

in geological mapping but provides very little information appropriate for mineral exploration. In the latter application in time decay rates are more valuable as the curves produced can be characteristic of specific types of conductor .

For example the decay curve of an isolated conductor in resistive medium shows a rapid decrease in amplitude in the 'early-time' stage but this changes to straight-line at late delay times. The gradient of this straight-line segment is used to derive a characteristic time constant ( $\tau$ ) when it is plotted logarithmically . These time constants are indicative of different types of causative bodies.

For mineral exploration, time constants in range 0.5-20ms are of particular interest. Pyrrhotite bodies often have very large time constants (several tens of milliseconds).

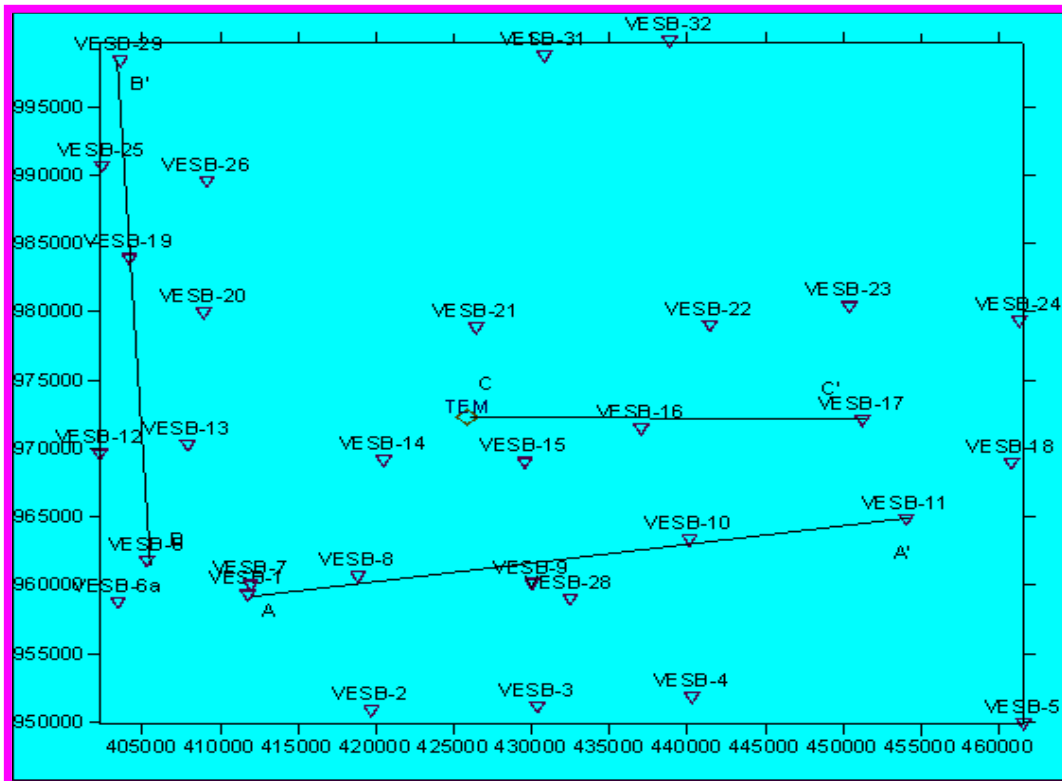
With the exception of nickel associations such targets are often of little economic interest. However time constants alone should not be used to attach either geological or economic significance to any particular target. The sense and degree of dip can be gauged from symmetry in measured components when plotted as a function of lateral distance long survey transverse lines.

While computer modelling is being used increasingly in the interpretation of data, classical inversion is notoriously difficult to apply to three dimensional models . Software for such processing is largely still research-based and requires inordinately long computer execution times on a mainframe computers. Consequently such processing has yet to be applied routinely to commercial TEM projects when three dimensional modelling is required . However for engineering and environmental applications, TEM sounding interpretation methods for wide variety of EM system have been given by Spies and Fuchs(1991) and Nabighian and Macnae(1991) among Others.

### 3.3 THE DISTRIBUTION OF TEM AND VES POINTS IN THE SURVEY AREA.

Figure 3.1 shows the distribution of the Vertical Electrical Sounding points used for both qualitative, semi-quantitative and quantitative analysis. In reference to this map, GPS measurement indicates that the nearest position to Addis Ababa is about 13.2Km, and the farthest is about 89.5 km. Moreover, Asgories is situated at about 57.1Km, from this survey area.

In Figure 3.1, the VES positions are marked by inverted triangles while the dark solid lines represent the imaginary profiles along which semi-quantitative analysis have been attempted



Scale: 1cm=5km

**Fig 3.1** The distribution of VES and TEM On the survey area

## CHAPTER FOUR

### 4. RESULT AND INTERPRETAION

#### 4.1 QUALITATIVE APPROACH

For a number of practical reasons, most geophysical data analysis and interpretations start, usually, from the qualitative view of the raw or semi-processed data. In case geoelectrical investigations, such approaches involves presenting the measured or computed apparent resistivity values as a function of:

- 1) lateral distances,
- 2) pseudo depths or
- 3) at their geographical position for a particular depth level.

In the first case, lateral distances, one has to define a known reference point and direction of advancement from which the horizontal variation in apparent resistivity can be shown on a simple line plot at an approximated depth level. This option is usually employed for data collected in a profiling modality.

In the second option, it is a common practice to plot the apparent resistivity from VES measurements, using the half electrode separation ( $AB/2$ ) as a pseudo depth values. The resulting plot is referred to as Pseudo-depth section and provides a 2D view, [ (X or Y) ,Z], of the resistivity variation with depth and along one of the lateral directions with respect to a known starting point.

The third option, at a single depth level shows the areal variation of the apparent resistivity of the ground section under question. Nevertheless, such presentations require adequate spatial coverage of the sounding points over the survey area.

At a particular virtual depth “ $AB/2$ ” level, the North-South and East-West variation of the measured apparent resistivities, systematically, reflects the directional dependence geo-

electrical parameters in a bi-dimensional plan map [X, Y]. When such maps are stacked at their respective depth order, they provide an additional dimension giving insight on the vertical stratification.

#### 4.1.1 Qualitative approach for the stacked plot

Figure 4.1 presents the regional variation of apparent resistivity from shallower level,  $AB/2=3\text{m}$  down to deeper horizons attained by  $AB/2=750\text{m}$ . All the 31 soundings are used for qualitative assessments of the electrical nature of the geologic medium.

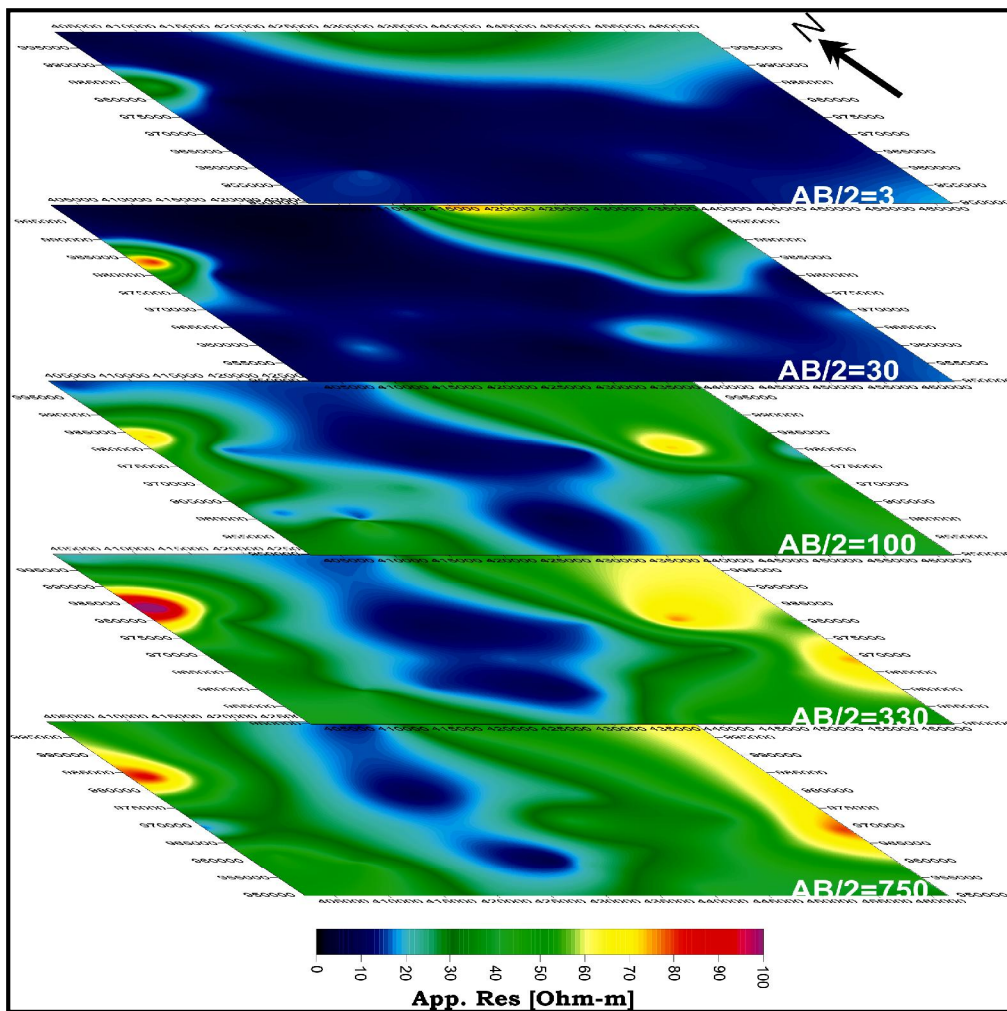


Figure 4.1: Stacked plan map of apparent resistivity of Becho plain

The sounding points are not evenly distributed and they are mainly concentrated in the central part of the area under investigation.

Referring to figure 4.1, the most notable feature on this stack plot is that the low resistivity zone, ( $< 20\Omega\text{-m}$ ), that occupy the vast portion of the survey area. The conductive region that is dominant over a wide area, at shallow depth levels, extends to the deepest level though its size decreases considerably.

On the other hand, the relatively higher resistivity responses, ( $> 40\Omega\text{-m}$ ) that are found in the northeastern and western borders of the study area, as narrow patches, ultimately broaden in areal extent with depth. Moreover, the amplitude of the resistivity response increases to  $70\Omega\text{-m}$  or more beyond pseudo depth of 330m in the eastern and northern border of the study area.

In consideration to the geology of the area described early in the introductory section of this document, the low resistivity region, in the vast central part of the shallower levels, seems to represent the alluvial zone.

The northern part of the survey area is described to be consisting of rhyolites, ignimbrites and subordinate trachytes. Moreover, Obsidian bearing rhyolites are known to be common in the northern part of the area under consideration. The relatively higher resistivity region shown at the northeastern flank of the stacked plan map could be the signature of these rock units on the surface. The above discussion shows that the regional resistivity image is in good agreement with the local geology.

#### 4.1.2 Qualitative interpretation of the lateral image at $AB/2$ equals 750m.

The last plate on the stacked plot of *Figure 4.1* depicts the response from deeper horizon. It is apparent that the central region is of anomalously lower electrical resistivity for such deeper ground. This feature may arouse a special interest from hydrogeological point of view.

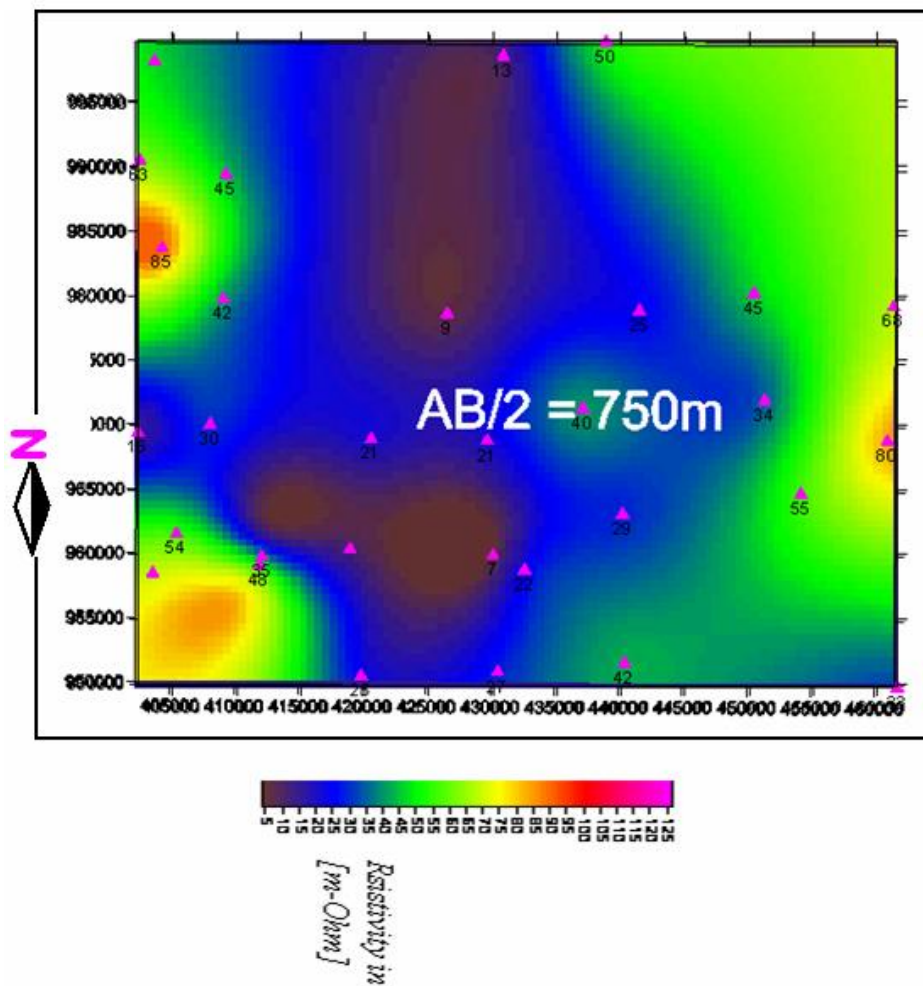


Figure 4.2: Apparent resistivity plan map at pseudo depth of  $AB/2 = 750m$ .

## **4.2 QUANTITATIVE AND SEMI-QUANTITATIVE INTERPRETATIONS.**

In geo-resistivity context, the major task in quantitative interpretation is analyzing the apparent resistivity succession, resulted from VES measurements, in terms of subsurface geoelectric layers defined by their respective true resistivities and thicknesses. The final analysis towards formulating a conceptual model involves designating these geoelectric layers to the likely geologic units.

The separations between the VES points employed in this thesis work are quite large and impede constructions of routine geoelectric sections for sound quantitative appraisal. Nevertheless, maximum effort has been made to make site-to-site correlations and come up with descriptive pictures of the subsurface along few profile lines.

### **4.2.1 Semi-quantitative interpretations of the 1-D geoelectric sections**

*Figure 4.3* shows the interpreted geoelectric stratification resulted from inversion of sounding data along profile AA'. This traverse represents the southern part of the study area and oriented in the roughly EW direction.

On this profile, more than four geoelectric layers are identified, with the exception under VESB1, where some additional thin layers have been encountered.

The first few meters of the ground is occupied by low resistivity layers, ( $< 15\Omega\text{-m}$ ), of variable thicknesses. These successions may represent top soils of varying composition and moisture content. The thickest portion of this soil cover is around mid position of A-A', at VESB10, and is about 13m. The thinnest soil layer is mapped at the eastern extreme position close to VESB11.

At depth, the eastern flank, VESB1 and VESB8, appears more resistive than the western flank, VESB10 and VESB11, and correlation along the entire traverse happens to be difficult.

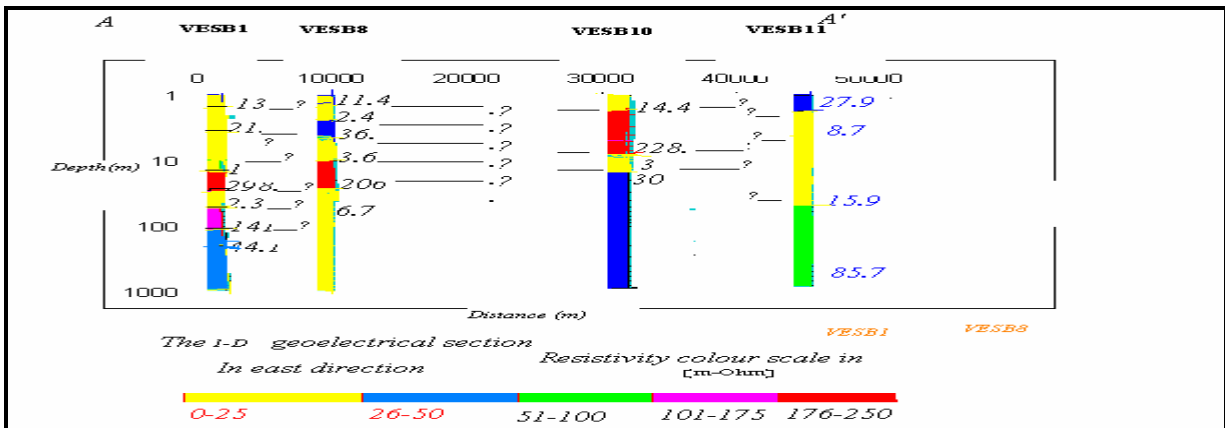


Figure 4.3, Interpreted geo-electric layers along profile A-A'

The interpreted geo-electric layers along profile BB' are shown on Figure 4.4. This line runs in NS direction along the western boarder of the study area. The line contains three soundings, namely VESB6, VESB19 and VESB29.

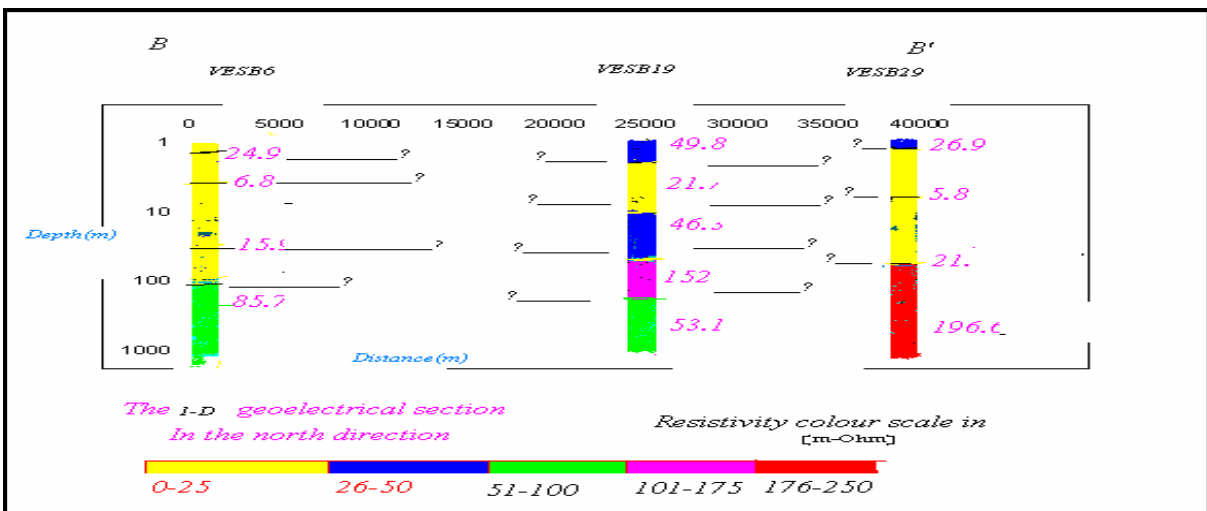


Figure 4.4: Interpreted geo-electric layers along profile B-B'

Four to five geoelectric layers are identified along this section. Unlike line A\_A', the first layer is relatively resistive, ranging from 25  $\Omega$ -m to 49.8 $\Omega$ -m. The thickness of this top soil layer

increases southward, from less than a meter at VESB29 to few meters at VESB6.

A conductive (5 – 20Ω-m) second and third layer, possibly representing the thick alluvial deposit, extend down to a considerable depth along this NS profile, though at VESB19 terminates shallower. The northern and central points, VESB29 and VESB19 mapped a resistive fourth layer with amplitudes in excess of 150Ω-m. The southern point VESB6, however, is underlain by a moderately resistive (~85Ωm) substratum. This same layer appears beneath VESB19 but, deeper than at VESB6. Figure 4.5: shows the geo-electrical picture of the subsurface under profile C-C’.

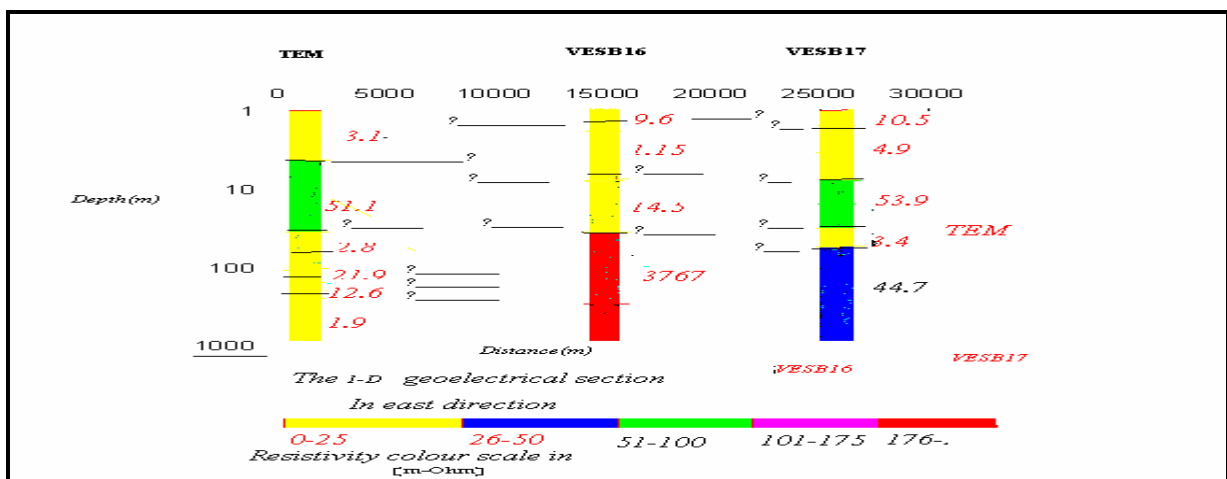


Figure 4.5: Interpreted geo-electric layers along profile C-C’

This geoelectrical picture is different from the above discussed, that it involves two VES soundings and one TEM in a single profile. Positioned at the center of the plain, the resistivity response is dominated by lower values down to a depth of more than 100m. Moreover, the stratification resulted from TEM sounding shows only the top conductive layers. This may be explained as the depth attained by TEM may not be compatible to the DC resistivity sounding owing to fast decay of the source signal in the conductive overburden.

### 4.3 THE OVERALL GEOELECTRIC PICTURE OF THE STUDY AREA

As a practical guideline for attributing the geoelectric layer to the geologic environment of the study area, the range of formation resistivities for the major lithological units in the study area are summarized in Table 4.1. The values are obtained from WWDSE’s database and were in-situ measurement by well-logging in existing boreholes in the region.

No	Estimated Resistivity range( $\Omega$ -m)	The main geological formation	Description	Remarks
1	2-20	Clay	Some times wet and weathered and interacted with silt	
2	20-90	Topsoil and unconsolidated Sediment	The unconsolidated sediment is comprised of sand, silt and gravel at place	This unit is occasionally water bearing
3	100-150	Acidic rock	Rhyolite,ignimbrite and trachyte wethered and fractured at places	Saturated and water bearing at places
4	150-250	Basic rock	Basalt which is fractured and weathered and sometimes scoraceous	Water bearing when it is fractured
5	250-500	Basic rocks	Basalt which is mostly fresh and unweathered	Dry to slightly water bearing

*Table 4.1, lithologic units and their resistivity ranges for Becho plain and the surrounding area, south-west Showa.*

Accordingly, the dominant three-to-four layer stratification, observed in the study area, can be attributed to top soil, unconsolidated sediments and sedimentary rocks of alluvial origins and volcanic substratum of acidic and / or basic composition.

# CHAPTER FIVE

## 5. CONCLUSIONS AND RECOMMENDATIONS

### 5.1 CONCLUSIONS

This study reveals that surface electrical measurements are effective to study ground water conditions. Based on the interpretation of geoelectrical data in conjunction with the geological information, the following conclusion can be drawn:

- The VES result reveals four subsurface geoelectrical layers; top soil covers, unconsolidated sediments and sedimentary layers of alluvial origin, and volcanic rocks.
- The alluvial deposit mainly consists of wet, weathered sand and intercalated with silt and clay dominates the mid position. The unconsolidated sediments in the eastern part are composed of gravel and sand with minor clay. As the resistivity values indicate, aquifer quality increases towards the east due to decreasing clay and favorable grain size.
- The volcanic rock may serve as aquifers but show different resistivity values depending on composition and degree of fracturing.
- The aquifer thickness increases towards both west and south.
- The average thickness of the saturated alluvium aquifer in eastern part has been estimated about 130m thick and the western part 230m.
- The boundary of the aquifer has been estimated and zones with high yield potential have thickness of aquifer were measure in east as 130m, 40thick mid position of WE ,20m west part ,NS 42m in mid position and 130m in the north extreme.High resistivity in the westrn part is due to the existence of alluvial fan that consist of a mixture of gravel,sand and silt.
- In the extreme part of SW part of survey area, we can note that aquifer is tilted to ward from northern part to southern part ,so it is possibly the source of artesian well (confined aquifer).

## 5.2 RECOMMENDATIONS

- It is preferable to use TEM and VES in the same sounding points.  
The reason is that VES can be used to fix the layer parameters for the top layers in the TEM version routine and TEM has higher resolution power than VES.
- TEM sounding and Profiles constructed should be closely spaced soundings in hydrogeology as most case histories demonstrated.
- To verify the estimated faults in the geoelectrical layers, gravity and magnetic methods is advisable to increase reliability of physical methods used.
- The dip and strike of this investigation can be used for further to determine the layers the hydraulic head and hydraulic gradient.
- It is better to consider the well site to be SW of survey area the reason is that, the most probable artesian aquifer can be obtained as shown in the Figure A.4.1 in SW of the survey area.
- The southern part is not good site for well site compare to SE and SW part. This part may be some time wet, weathered and interacted with very low resistivity area.
- In general, the survey area may be considered as important source of ground water. The reason is that all geophysical methods used, indicate low resistivity of subsurface (rocks) which is characteristic of porosity (fracture) and water saturation or its salt content. So it is better to continue further study to the objective of the project.

## References

- Bhattacharya, P.K., and Patra, H.P.,1968. Direct current geoelectrical sounding, Elsevier, Amsterdam.
- Davis and Dewiest. Hydrogeology ,1<sup>st</sup>Edition.John Wiley and sons,Inc.,1966.
- D.H.Griffiths and R.F.King.Applied Geophysics for engineering and geologists,1<sup>st</sup> Edition. Pergamon Press,1965.
- Deppermann,K.,1954.Die Abhangigkeit descheinbaren Widerstandes vom Sondenabstand bei der Vierpunkt-Methode.Geophysics prospecting2,p.262-273.
- Dodds,A.R., and Ivic,D.1990.Integrated geophysical methods used for ground water studies in the Murray basin, South Australia in Geotechnical and Environmental Geophysics
- Fitterman, D.V., and M.T. Stewart, Transient Electromagnetic sounding for ground water, Geophysics, 51,995-1005, 1986.
- Frischt,1991.Electromagneticsounding.In:Nabighian,M.N.edElect.Meth. Apply.Geophysics, 2, Application, PartA, 285-386, Soc.Explor.Geophysics.
- Ghosh, D.P., 1971a.The application of linear filter theory to the direct interpretation of geoelectrical resistivity sounding measurements, Geoph.Prosp.19, p192-217.
- Ghosh, D.P.,1971b. Inverse filter coefficients for the computation of apparent resistivity standard curves for a horizontally stratified earth, Geoph.Prosp.19, p.769-775.
- Ghosh,D.P.,1970.The application of linear filter theory to the direct interpretation of geoelectrical resistivity measurements Ph.D. Published.
- John M.Rnolds .Anintroduction to applied and enviromrntal geophysics,1<sup>st</sup> Edition.JohnWiley and Sons Ltd, 1997.
- K.-M.Strack.Exploration with deep transient electromagnetics, 2nd Edition. Elsevier Science Publisher B. V,1992.
- Kazmin,V.1979:Geology of Ethiopia Explanatory notes to Geological Map of Ethiopia1:2,000,000,Ethiopia institute of Geological survey
- Mohr, P.A.1961, 1964 and 1979: The geology of Ethiopia,HaillessilaseI University Press Addiss Ababa.

M.S.Zhanov and G.V.Keller.The geo electrical methods in geophysical exploration,2<sup>nd</sup> Edition.Elsevier Science Publisher B.V.,1998.

Nabighian,M.N.and J.C.Macnae, 1991.Time domain electromagnetic prospecting methods.In:Nabighian, M.N.,Ed Electromagnetic methods in applied geophysics.

Orellana, E.andMooney,H.M.,1966.Master tables and curves for electrical sounding over layered structures,Intercientia,Madrid.

Paranis, D.S. Minig Geophysics.Methuen and Co.Ltd, London, 1973.Spies, B.R. and F.C.

Plummer, McGear, Carlson.Physical geology, 8th Edition. Edward E.Bartell, 1999.

Shabtaie,S.,Bentley,C.R.(1982) Deep geoelectric and radar soundings at Dome C geophysical survey.AntarcticJournal of the unite States,**15**(5):2-5

Shabtaie,S.,Thyssen,F.andBentley,C.R.(1982) Deep geoelectric and radar soundings at DomeC,East Antarctica.Annals of Glaciology,**3**:342

Sri Niwas and Israil,M.(1986):Computation of apparent resistivities using an exponential approximation of kernel function.

Stefansescu,S.S.(1930) : sur la distribution electrique avtour d'une prise deterre ponctuelledoms un terrain acounha horizontals homogenes et isotrope,*J,phys-paris*,7,series1.

Stephanetal (1991): Data processing sequence for 'long off set transient' (LOTEM) sounding in Germany.

Taylor, K., et al.Use of transient EM to define local hydrologeology in arid and alluvium environmental geophys, *57*, 343, 1992.

Telford, W.M, and Others.Applied geophysics.Cambrige university press, 1976.

Water Works Design and Supervision Enterprise, 2008.Adaa and Becho plain ground water resources development and irrigation project.

Zohdy,A.A.R.,1965. The auxiliary point method of electrical sounding interpretation and its relationship to the DarZarrouk parameters:Geophysics,v.30,no.4,p.644-660.

## DECLARATION

I declared that this thesis original work is mine and has not been presented for a degree in other university and all sources of relevant materials such as books and articles, etc., have been duly acknowledged.

Name

Birhan Muche

Signature

\_\_\_\_\_

Place and Date of submission:

Addis Ababa,

7/20/2008

This thesis has been submitted for examination with my approval as University Advisor.

Name : Dr. Shimeles Fisseha

Signature: \_\_\_\_\_

# ANNEX

## **A.1 MEASURING THE CURRENT PENETRATION DEPTH**

## **A.2 THE 3-D GEOELECTRICAL SECTION FOR THE RESPECTIVE FOUR LAYERS**

## **A.3 QUANTITATIVE AND SEMIQUANTITATIVE INTERPRETATION TEM**

## **A.4 QUANTITATIVE AND SEMIQUANTITATIVE INTERPRETATION THE SUBSURFACE LAYERS IN 3-D GEOELECTRICAL SECTIONS OF VES**

## **A.5 THE 2-D GEOELECTRICAL SECTION**

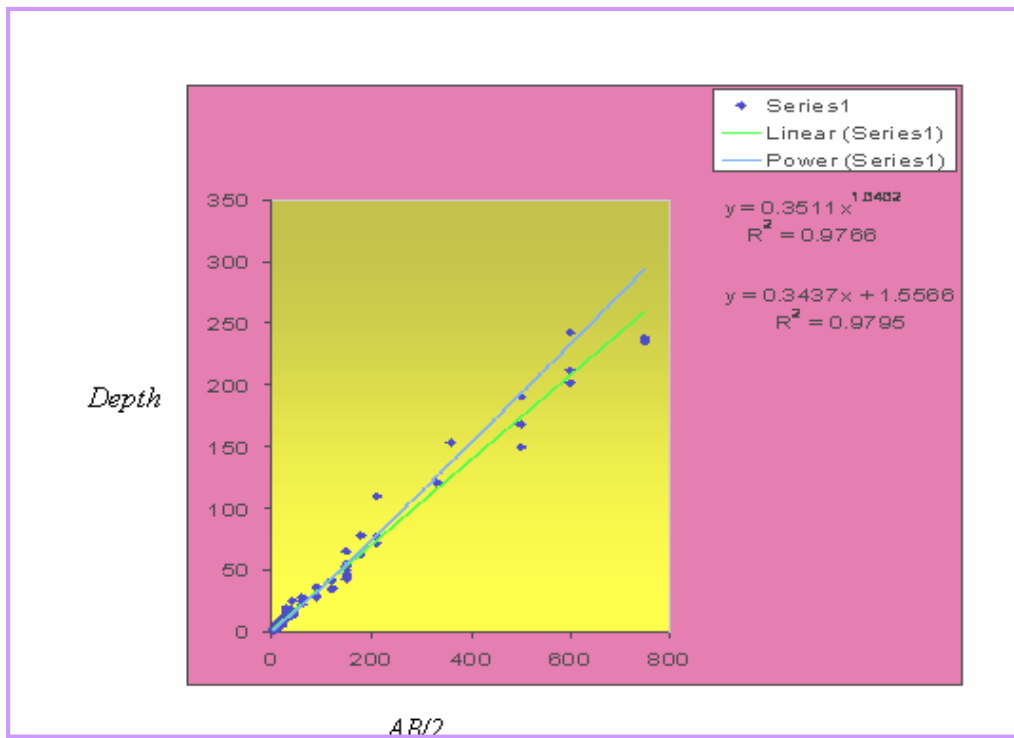
## **A.6 GLOSSARY**

### **A.5.1 Geophysics terms**

### *A.5.2 Hydrogeological concepts and terms*

## **west A.7 THE INVERTED DATA PLOTS AND THEIR CORRESPONDING RESULTS**

## A.1 MEASURING THE CURRENT PENETRATION DEPTH



*FigA.1.1:Correlation between depth of current penetration and current electrodes spacing AB/2*

Note: Even though we use linear regression, we have a priore information about the current penetration. This result indicates that the current depth penetration is given by  $AB/5$

## A.2 THE 3-D GEOELECTRICAL SECTION FOR THE RESPECTIVE FOUR LAYERS

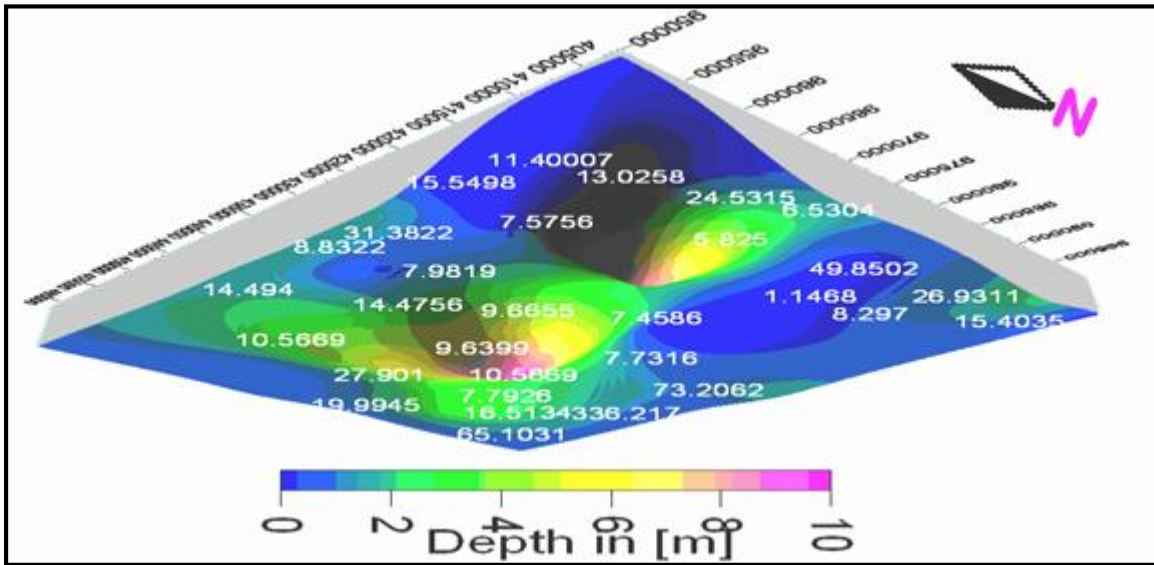


Fig A.2.1: The 3-D geoelectrical section of the first layer.

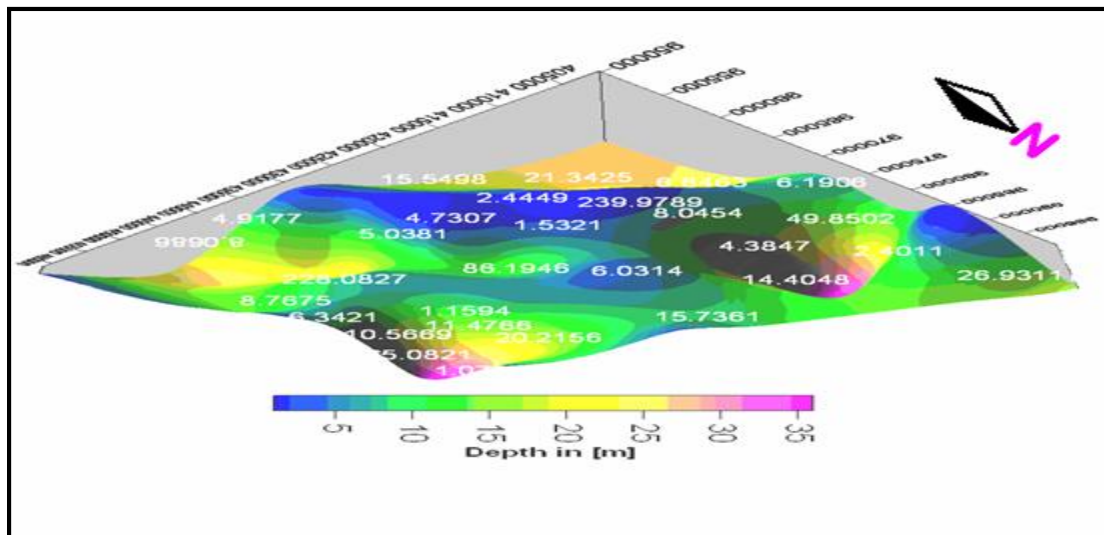


Fig A.2.2: The 3-D geoelectrical section of second layer.

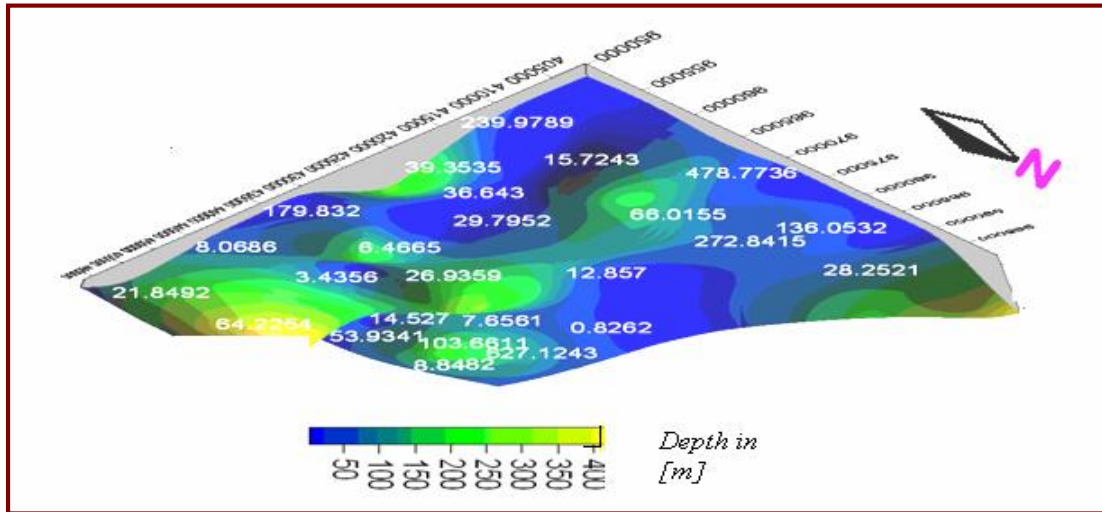


Fig A.2.3: The 3-D geoelectrical section of the third layer

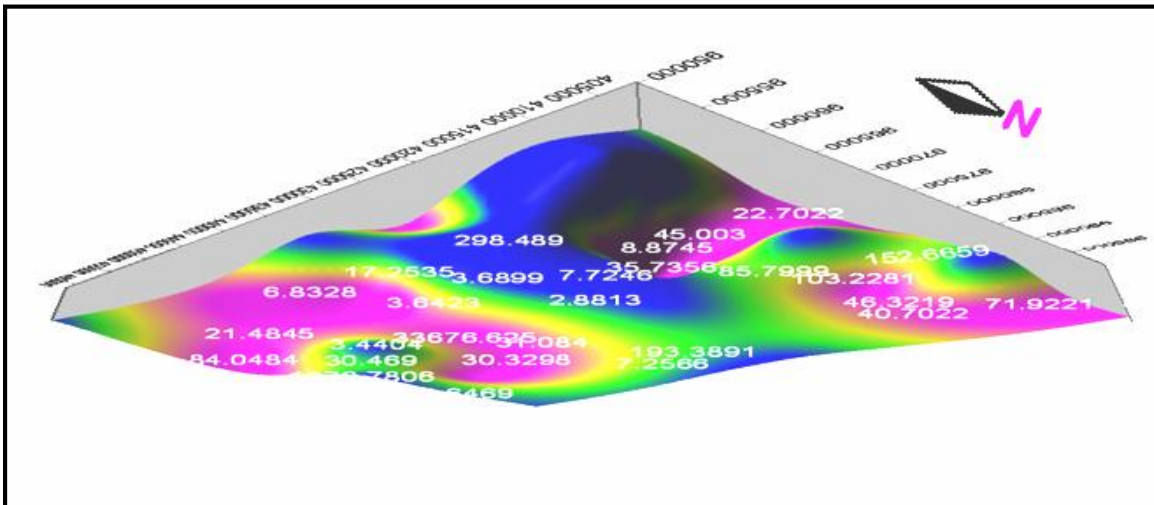


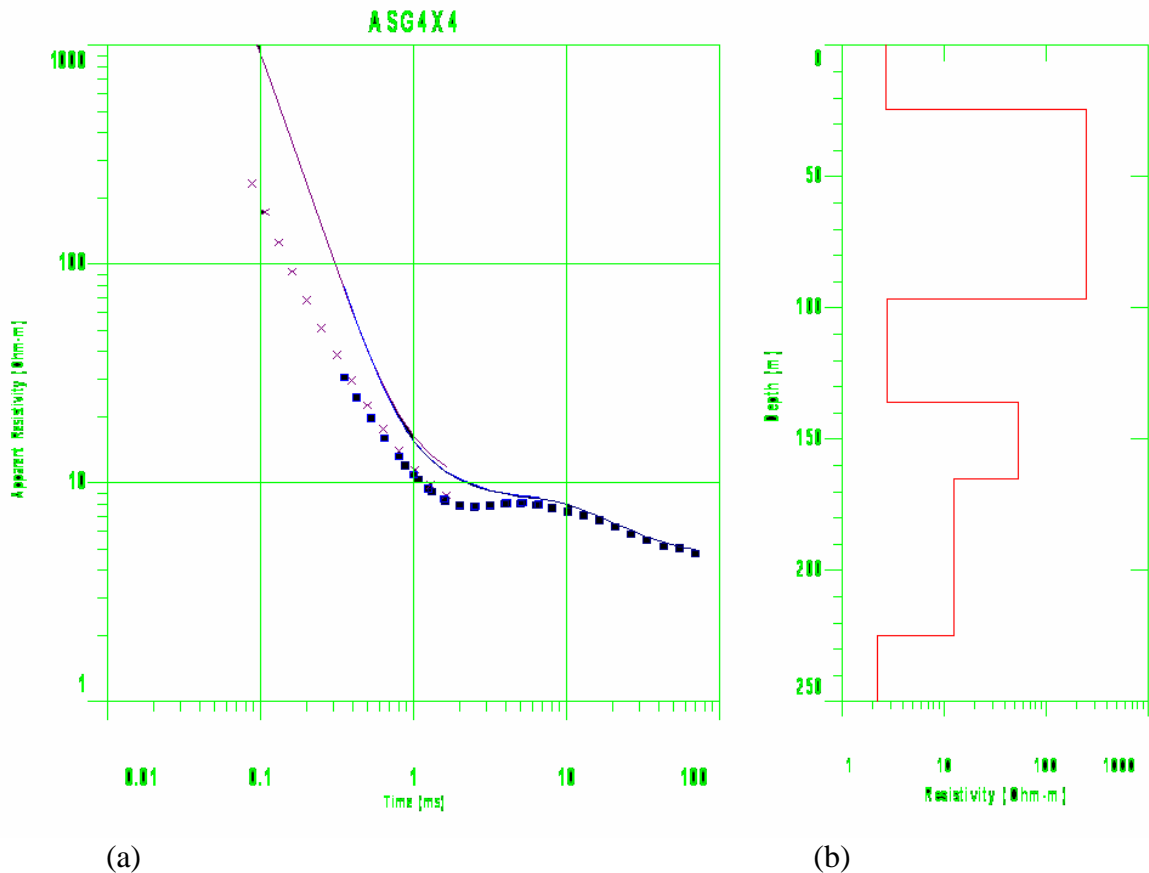
Fig A.2.4: The 3-D geoelectrical section of the fourth layer

Depth (Infinite depth).

### A.3 QUANTITATIVE AND SEMIQUANTITATIVE INTERPRETATION TEM

Fig A.3.1 shows the 1-D geoelectrical section, its depth varies from 25m to 225m and the range of its resistivity is  $49\Omega\text{-m}$  that is it varies from  $2\Omega\text{-m}$  to  $51\Omega\text{-m}$ . This geoelectrical section identified as six layers. The first layer depth is 24.4m and the second layer depth is 95.1m. This is quite different from VES result even if we consider VESB15 its first layer depth is 9m and the second layer depth is 12.6m. This result should not confuse as because the VES inversions were then used to fix the layer parameters for the top layers in the TEM inversion routine [Dodds and Ivic, 1990].

In addition, this method helps us to identify the presence of thin layers as its resolution is higher compare VES method that is under the above top layers, other four layers are identified with 226m depth. From this result, TEM is preferable to identify thin layers for this study area



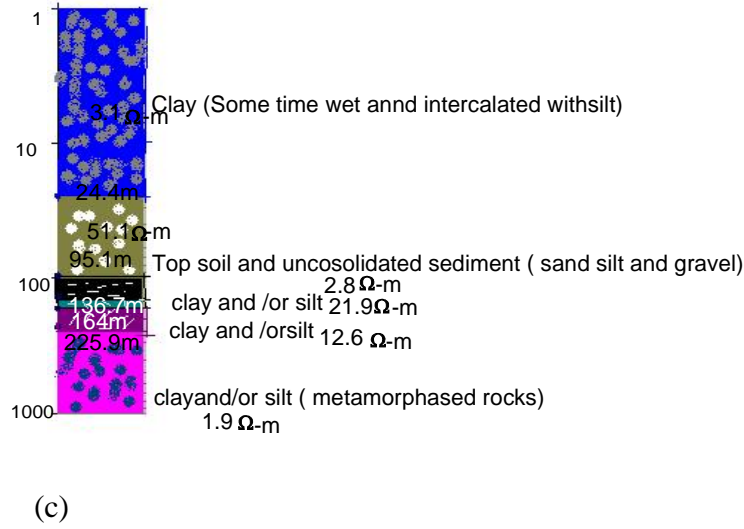
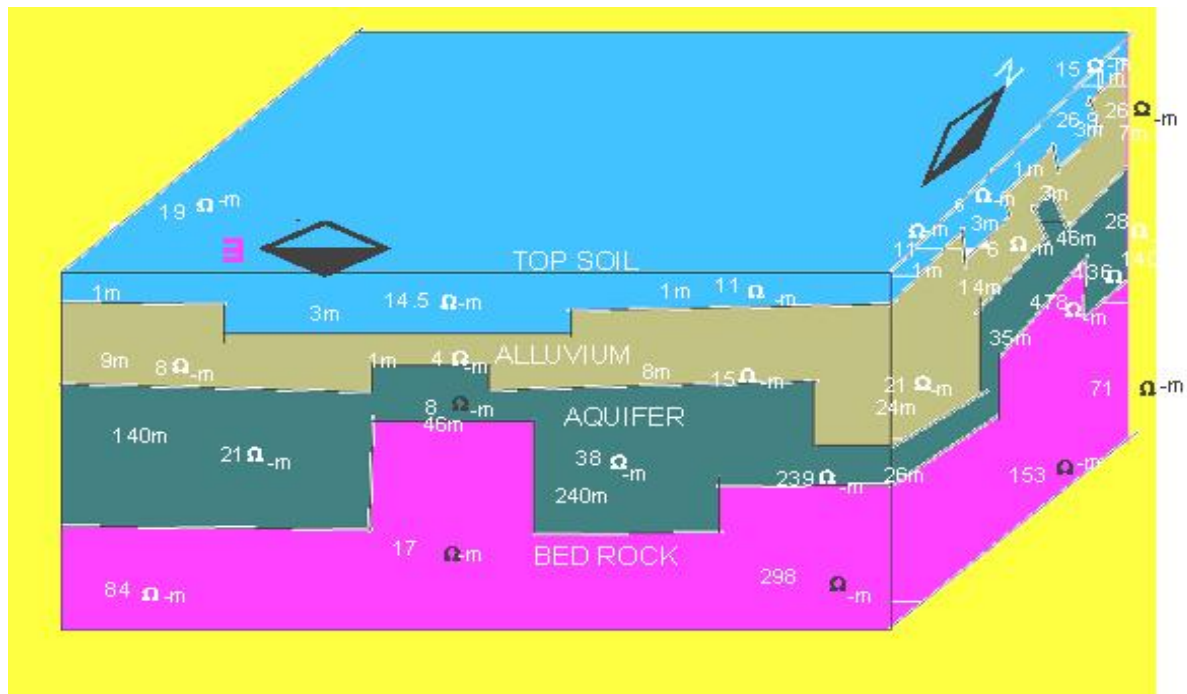


Fig A.3.1 (a) apparent resistivity versus delay time (b) 1-D geoelectrical section of inverted result of (a) and (c) the corresponding geological interpretation of TEM.

#### A.4 QUANTITATIVE AND SEMIQUANTITATIVE INTERPRETATION THE SUBSURFACE LAYERS IN 3-D GEOELECTRICAL SECTIONS OF VES

Based on 3-D geoelectrical sections in figures shown above, Figure A.2.1-A.2.4, It is possible to construct the sub surface layering NS and EW, which can show part of the aquifers, their thickness and resistivity values. The aquifer consists of two main western and eastern parts that is separated in the mid position along with the Stacked image plot depth section anticipation. The thickness of the aquifer and depth of the bed rocks is different in the two parts.

The resistivity of the thin top layer, alluvium, aquifer and bed Bedrocks values are shown in Fig A.4.1. These data indicate that the bed rock in both sides of the aquifer is different and the bed rock intruded in between the aquifer is electrical low resistivity zone. It is possibly a weak zone and there may be a fault, which is consistent with the pseudo depth stacked section interpretation in the SN direction.



*Fig A.4.1: Sub surfacelayers in NS and WE parts of the aquifers, depth and resistivity values are given in this plot.*

## A.5 THE 2-D GEOELECTRICAL SECTION

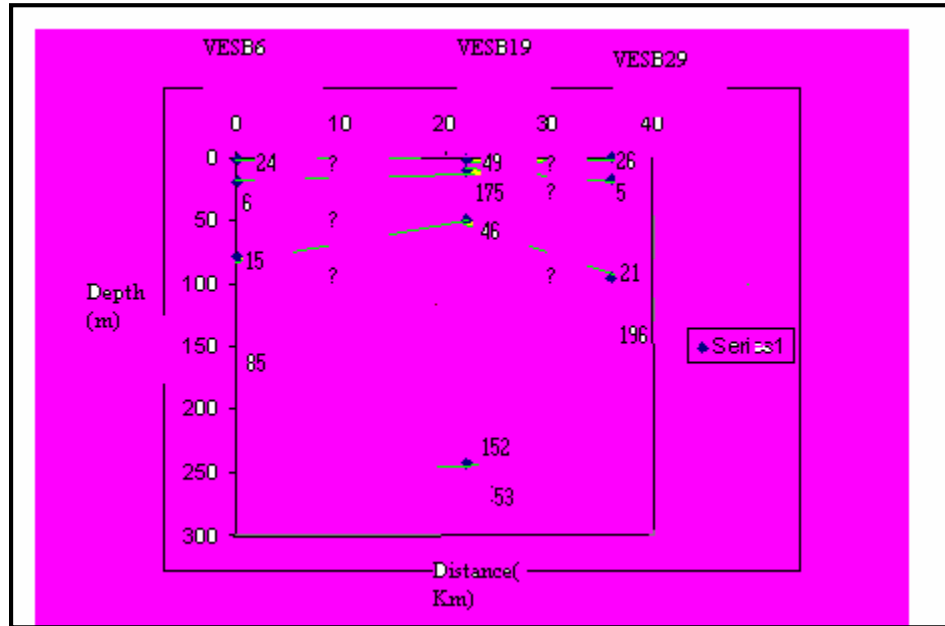


Figure A.5.1: Along the profile B-B'

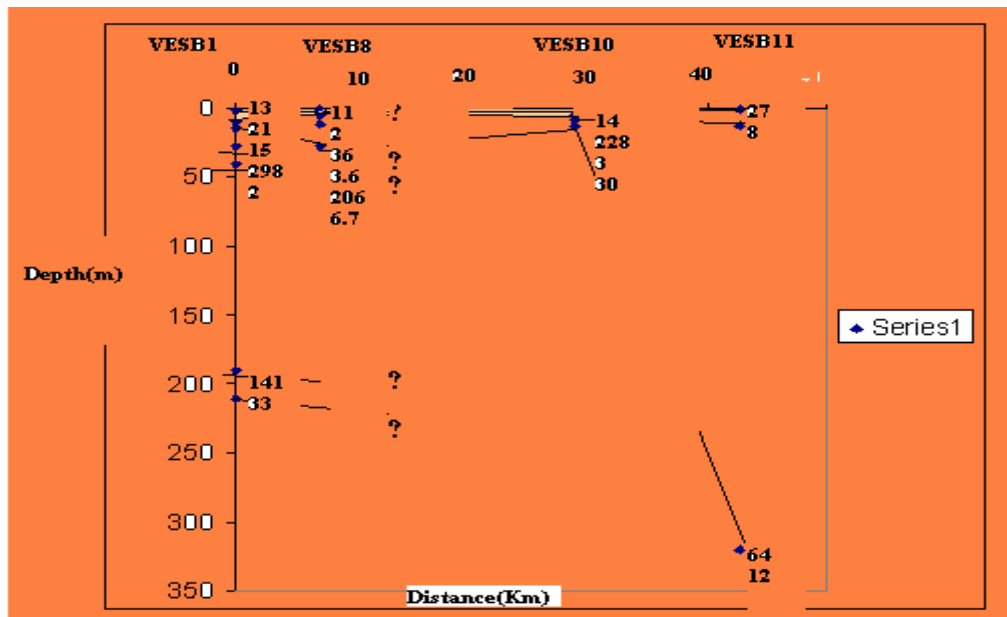


Figure A.5.2: Along the profile A-A'

## A.6 GLOSSARY

### A.6.1 Geophysics terms

**Controlled source electromagnetics:** a terminology grouping all electromagnetic techniques which use their own transmitter. Examples are transient and controlled source audio EM (CSAMT).

**Cultural noise :** electromagnetic noise caused by man and the effect of industrialization (i.e. Power lines)

**Inversion :** a procedure to derive from the field data an earth model which is consistent with the data and describe the subsurface.

**Joint inversion :** when inverting two independent data sets simultaneously to obtain one resulting model, one calls this process joint inversion. Usually the data vector has the length of both datasets while the model parameter vector remains the same length as for ordinary inversion methods.

**LOTEM :** Long Offset Transient Electromagnetic. A transient electromagnetic sounding technique using an earthed wire transmitter and several components of the electromagnetic field at receiver which yields independent information on the resistivity structure of the subsurface

**Notch filter :** a filter that passes all frequencies except those in a stop band centered on a center frequency.

**Offset :** distance between transmitter and receiver center position

**SIROTEM:** shallow transient EM system developed by Scientific and Industrial Research Organization of Australia.

**Ramp time :** the time the transmitter current requires to go from one constant state to the other.

## ***A.6.2 Hydrogeological concepts and terms***

**Alluvial fan :** As river emerges from the mountains on flatten plains,they deposit broad,fan-shaped piles of sediment.The sediment often consist of coarse,arkosic sandstones and conglomerates,marked by coarse cross-bedding and less-like channel deposit.fan or cone-shaped pile of sediment that usually forms where a stream velocitydecreases as it emerges from anarrow mountaintcanyon on to the flat plain.

**Aquifer:** abody of saturated rocks or sediment through which water can move easily,aquifer are both high permeable and saturated water.

**Aqitard:** rocks or sediments those cause retard of the flow of ground water **Artesian well:** confined aquifer,it is tilted and exposed to erosion.

boulder (256mm), cobble (64mm),pebble(2mm),Breccia(angularparticle) and conglomerate(rounded particles)

**Clay:** finest sediment less than 1/256 mm too fine to feel gritty to finger or teeth.

**Delta:** a body of sediment depositat mouth of ariver when river velocity decreases,represent Greek letterdelta 'Δ' triangular.

**Dike:** tabular (shaped tabletop) discordant intrusion.Discordant means that the body is not parallel to any layering the country rocks.

**Fault :** a fracture in the bed rocks along which movement has taken place.

Gravel includes all rounded particles coarser than 2mm in diameter.This include the term

**Mud :** a term loosely used for wet silt and clay. Mud may silt (mostlysiltor shale) or mud stone Cmostly clay).

**Sand:** grain from1/16 mm(about athickness of our hair) to 2mm.

**Shale :** afine-grain sediment that is sedimentary rock notable for its capability(called fissibility),splitting takes place along the surfaces of very thin layer (laminations) with in ashale. Most shales-contain both silt and clay (average 2/3 claysized mineral, 1/3 silt sized quartz) and are so fine –grained that surface of the rock very smooth.

**Sill:** also a tabular intrusion structure but it is concordant,that is sills un like dikes are parallel to any planes,laying in the country rocks.

**Silt :** its size from 1/256 mm to 1/6mm and does not feel gritty between figures.

**Slate:** a very thin grain rock with an earth luster,splits easilyin to athin,flat sheet.

In 1856 **Henry Darcy**, a French engineer, found that the velocity at which ground water moves depends on the **hydraulic head** of water and up on the permeability of the material that water is moving through.

The hydraulic head of a drop of water is equal to the elevation of drop plus the water pressure on the drop.

$$\text{Hydraulic head} = \text{elevation of the drop} + \text{pressure of the water on drop}$$

Hydraulic gradient is the difference in head between two points divided by the distance between them.

$$\text{Hydraulic gradient of the drop} = \left( \frac{\text{difference hydraulic head of drops at different position}}{\text{distance}} \right)$$

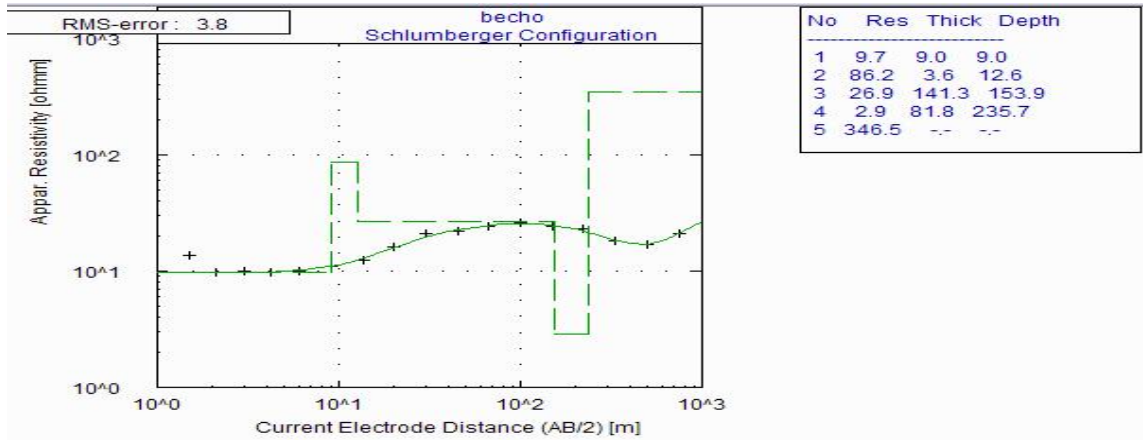
Note that underground water may move down ward ,horizontally,or upward in the response to differences in the hydraulic head,but that it always moves in the direction of downward slope of the water table above it.

Darcy found the velocity of ground waterflow is caused by both the permeability of sediment or rock and hydraulic gradient of water.

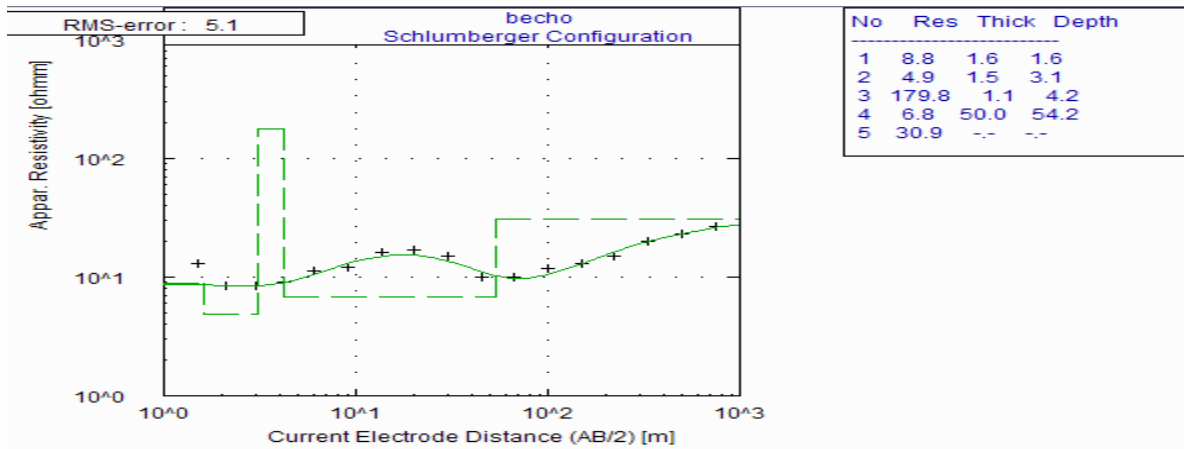
$$\text{Velocity} = \text{permeability} \times \text{hydraulic gradient}$$

$$V = K \left( \frac{\text{hydraulic head}}{L} \right), \text{ where } K \text{ is the hydraulic conductivity; it is the measureability.}$$

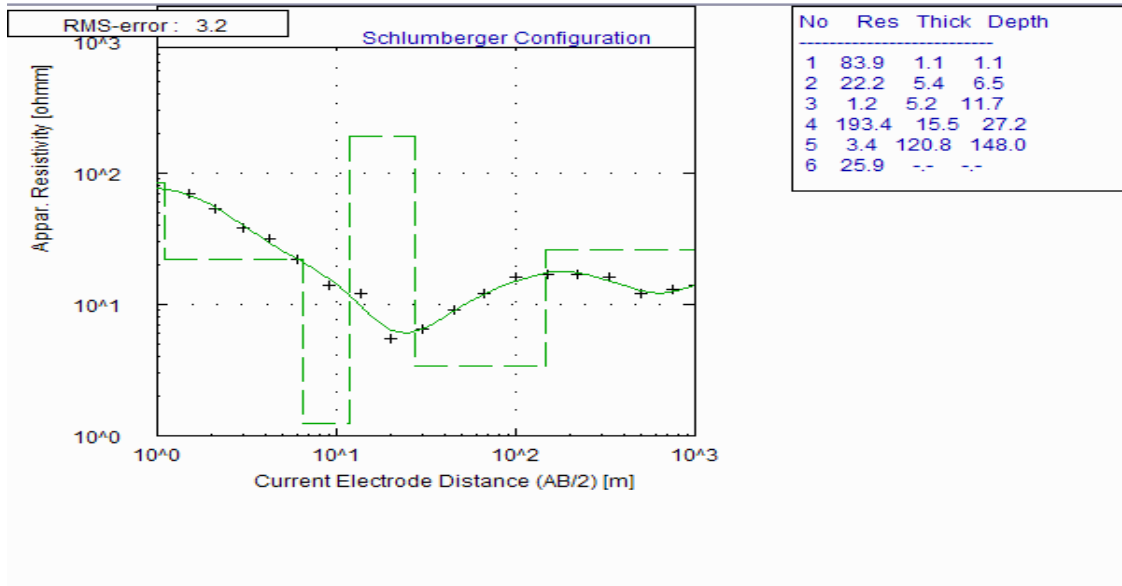
# FIGURE A.7 THE INVERTED DATA PLOTS AND THEIR CORRESPONDING RESULTS



## VESB3



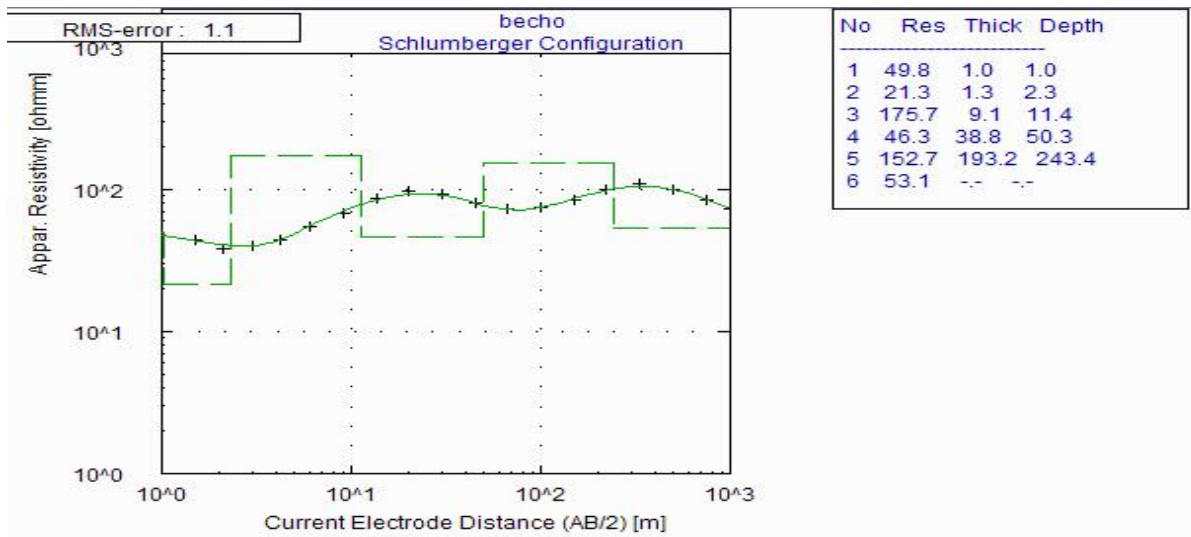
## VESB15



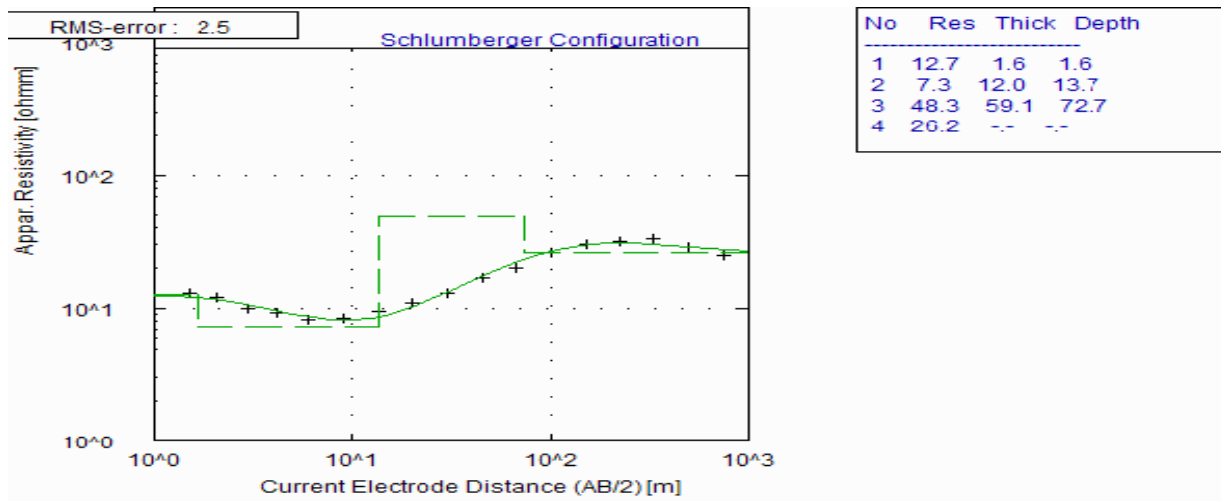
VESB31



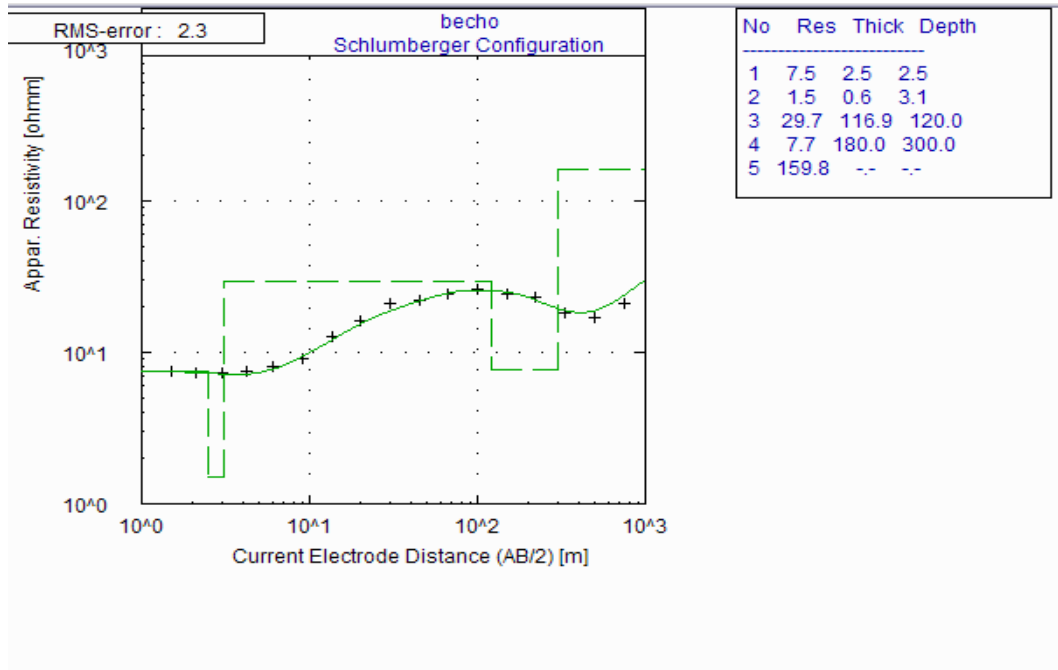
VESB9



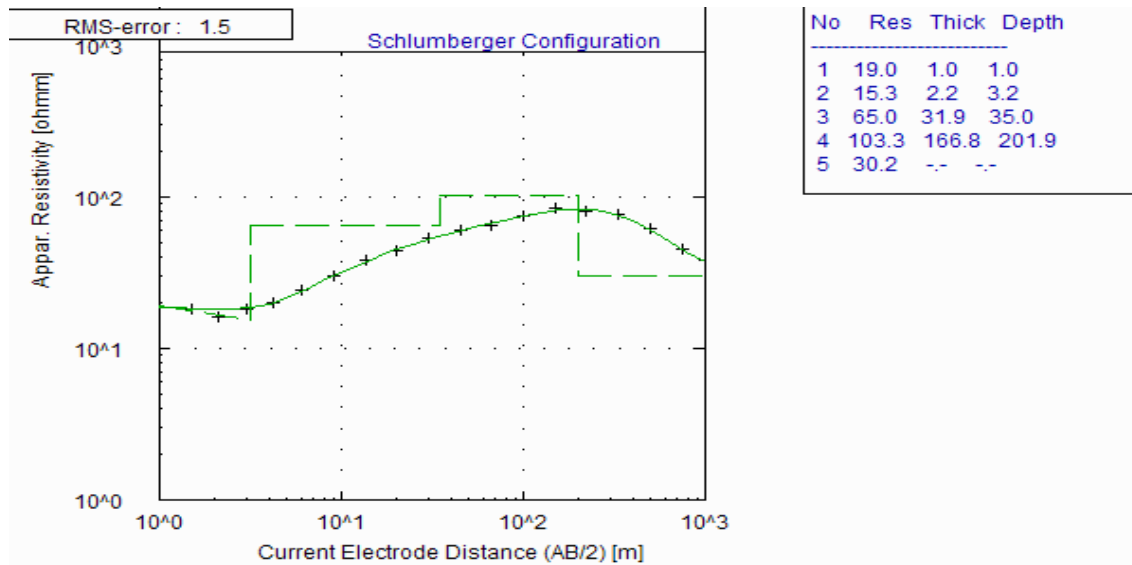
VESB19



VESB2



### VESB1



### VESB23